

CoSpaDi: Compressing LLMs via Calibration-Guided Sparse Dictionary Learning

 **Denis Makhov**¹ **Dmitriy Shopkhoev**^{1,2}
Magauiya Zhussip¹ **Ammar Ali**^{1,2} **Stamatios Lefkimiatis**¹
Fundamental Research Center
MWS AI¹, ITMO²

Abstract

Post-training compression of large language models (LLMs) often relies on low-rank weight approximations that represent each column of the weight matrix in a shared low-dimensional subspace. This strategy is computationally efficient but the underlying constraint can be overly rigid for heterogeneous projection weights and may incur avoidable accuracy loss. We propose **CoSpaDi** (Compression via Sparse Dictionary Learning), a training-free framework that replaces low-rank factorization with a structured sparse decomposition in which each weight matrix is represented as a dense dictionary multiplied by a column-sparse coefficient matrix. This yields a union-of-subspaces model: the columns of the weight matrix are represented as linear combinations of different subsets of dictionary atoms, improving expressiveness at a fixed parameter budget. CoSpaDi is *calibration-guided*: using a small calibration set, we optimize the factorization to minimize functional reconstruction error of layer outputs rather than weight-space error. An activation-derived Gram orthonormalization reformulates this data-aware objective into a standard dictionary learning problem on transformed weights, and we support both per-layer compression and cross-layer dictionary sharing within groups of similar projections. Across Llama and Qwen model families, CoSpaDi consistently improves the accuracy–compression and perplexity–compression trade-offs over state-of-the-art SVD-based baselines and strong structured pruning baselines at 20–40% compression ratios. The resulting structured sparsity enables sparse–dense computation and integrates with post-training quantization of the sparse coefficients.

1 Introduction

Large language models (LLMs) achieve strong performance across diverse tasks, from dialogue and instruction following (Brown et al., 2020; Achiam et al., 2023) to general-purpose reasoning (Touvron et al., 2023; Anil et al., 2023). Their effectiveness stems in part from their Transformer-based architectures that model long-range dependencies with attention (Vaswani et al., 2017; Devlin et al., 2019). At the same time, the scale that enables these capabilities makes LLMs expensive to store and run, creating a practical barrier to deployment on memory- and compute-constrained hardware.

A broad literature addresses post-training compression and acceleration of LLMs, spanning pruning, quantization, knowledge distillation, and structured weight parameterizations such as matrix factorization (Frankle & Carbin, 2019; Dettmers et al., 2022; Hinton et al., 2015; Denton et al., 2014). Among training-free approaches, matrix factorization is particularly attractive because it yields explicit low-parameter surrogates for large projection matrices, and in practice the predominant choice is truncated SVD and its activation-aware variants that use a small calibration set to guide which components to keep and how to scale them (Chen et al., 2021). Cross-layer extensions further reduce overhead by sharing a common low-dimensional subspace across groups of layers (Wang et al., 2025a). Despite strong results, these methods ultimately approximate each matrix within a *single* shared low-dimensional subspace; for heterogeneous Transformer projections, this constraint can be unnecessarily restrictive and motivates richer factorizations.

We study an alternative factorization family that relaxes this constraint. Instead of approximating a matrix with one global low-dimensional basis, we model it using a *union of subspaces* via sparse dictionary learning (Aharon et al., 2006; Elad, 2010): a learned dictionary of atoms is combined with column-sparse coefficients, allowing different columns to be reconstructed from different subsets of atoms. This representation is more flexible than a single shared subspace at the same parameter budget, and it is well aligned with the intuition that different output channels may depend on different latent features.

Building on this idea, we propose **CoSpaDi** (Compression via Sparse Dictionary Learning), a training-free compression framework for Transformer projections. CoSpaDi learns dictionaries and sparse codes to approximate pretrained weight matrices, and is *data-aware*: from a small calibration set we construct an activation-derived Gram orthonormalization that reformulates functional output reconstruction into a standard dictionary learning problem on a transformed (activation-weighted) weight matrices. The resulting factorization yields structured sparsity that can be paired with post-training quantization of the sparse coefficients, and it naturally supports both *per-layer* compression and *cross-layer* dictionary sharing for groups of related projections.

Contributions.

- **Beyond low-rank for post-training compression.** We introduce sparse dictionary learning as a compression paradigm for LLM weight matrices, replacing the single-subspace constraint of SVD-based factorization with a union-of-subspaces representation.
- **Calibration-guided, training-free optimization.** We integrate sparse dictionary learning with a data-aware objective via activation-derived Gram orthonormalization, yielding a tractable transformed problem that can be optimized efficiently with alternating sparse coding and dictionary updates, without gradient-based fine-tuning.
- **Empirical gains across settings.** Across multiple Llama and Qwen models and a range of compression ratios, CoSpaDi improves the quality–compression trade-off over strong activation-aware SVD baselines (including SVD-LLM (Wang et al., 2025c) in the per-layer setting and Basis Sharing (Wang et al., 2025a) in the grouped setting), and is competitive with recent structured pruning methods (Ma et al., 2023; Shopkhoev et al., 2025).

2 Related Work

Post-training compression for Transformers is commonly organized around *what is preserved* (weights, activations, or end-to-end behavior) and *what structure is imposed* (sparsity, low precision, low rank, or shared components). We review the most relevant directions through this lens, and position CoSpaDi as a functional, calibration-guided method that imposes a union-of-subspaces structure via sparse dictionary learning.

Post-training pruning and practical sparsity. A central theme in recent LLM compression is to optimize a compressed representation to match layer outputs on a small calibration set, rather than minimizing weight-space error. This perspective appears prominently in one-shot *unstructured* pruning methods such as SparseGPT (Frantar & Alistarh, 2023) and its simplified activation-driven variants (e.g., Wanda) (Sun et al., 2024), which induce high sparsity with limited degradation by explicitly targeting output preservation. However, unstructured sparsity does not automatically translate into practical *compression* or *speedups*: sparse storage formats typically require additional metadata (e.g., indices in CSR/CSC-like representations), which can substantially reduce effective memory gains at moderate sparsity, and irregular access patterns often make sparse matmuls memory-bound and kernel-limited (Han et al., 2015; Wang, 2020). In practice, inference acceleration usually benefits most from *structured* sparsity patterns and dedicated kernel/hardware support (e.g., 2:4 sparse tensor cores) (Mishra et al., 2021; NVIDIA, 2020). Complementary structured approaches remove or replace higher-level components (blocks/layers) using importance criteria and brief recovery steps (Ma et al., 2023; Shopkhoev et al., 2025). Our work follows the same calibration-guided spirit, but instead of removing weights, we seek a structured factorization that can represent heterogeneous columns more flexibly than a shared low-dimensional subspace.

Quantization and equivalent transformations. Quantization reduces memory footprint and can improve throughput, but accuracy at low bit-width often hinges on handling outliers and reshaping activation/weight distributions. Weight-only PTQ methods include vector-wise quantization with outlier routing (Dettmers et al., 2022), Hessian-aware schemes such as GPTQ/OPTQ (Frantar et al., 2023a;b), and activation-aware scaling/outlier protection (Lin et al., 2024; Dettmers et al., 2024). For weight-and-activation quantization, methods such as SmoothQuant (Xiao et al., 2023) and rotation-based transforms (e.g., QuaRot) (Ashkboos et al., 2024) improve quantizability by rebalancing channel ranges or suppressing outliers. These techniques are complementary to structural compression: in our setting, the sparse coefficients produced by CoSpaDi can be quantized post hoc to further reduce memory and potentially improve practical efficiency.

Low-rank factorization and shared subspaces. A widely used post-training alternative to pruning is matrix factorization, where each projection is approximated with a low-rank surrogate (Denton et al., 2014). Activation-aware and functional variants include DRONE (Chen et al., 2021), Fisher-weighted reconstruction (FWSVD) (Hsu et al., 2022), and adaptive truncation with activation transforms (ASVD) (Yuan et al., 2023). More recent SVD-LLM methods incorporate truncation-aware whitening and improved allocation strategies across layers (Wang et al., 2025c;b; Qinsi et al., 2025). In parallel, Basis Sharing (Wang et al., 2025a) ties factors across layers to exploit inter-layer redundancy. While effective, these approaches still represent each matrix in a *single* shared subspace (possibly partially shared across layers). Our method targets the same post-training regime, but replaces the single-subspace constraint with a union-of-subspaces representation enabled by sparse coding.

Dictionary learning and sparse representations. Dictionary learning and sparse coding have a long history in signal processing and vision (Engan et al., 1999; Aharon et al., 2006; Mairal et al., 2009; Gregor & LeCun, 2010; Elad, 2010), where they provide expressive, parsimonious representations that adaptively select a small subset of atoms per example. In model compression, related ideas appear in structured decompositions such as GroupReduce (Chen et al., 2018) and tensorized factorization schemes (Ma et al., 2019). Recent work has also applied learned dictionaries to other Transformer components, e.g., KV-cache compression via sparse decoding (Kim et al., 2025), and cross-layer sharing formulations specialized to attention (Zhussip et al., 2025), which connects to broader shared-basis approaches (Wang et al., 2025a). In contrast, our focus is a *training-free, calibration-guided* dictionary learning framework for *weight* compression that (i) explicitly optimizes a functional objective through activation-aware Gram orthonormalization, and (ii) supports both per-layer compression and cross-layer dictionary sharing within a unified procedure.

3 Method

We first formulate post-training compression objectives in *weight space* and *activation space*. We then reinterpret truncated SVD through the lens of PCA as a “basis times coefficients” model, and introduce sparse dictionary learning as a more expressive union-of-subspaces alternative. Finally, we describe CoSpaDi and its grouped extension, together with compression and complexity estimates.

3.1 Problem formulation: weight-space vs. activation-space objectives

Consider a pretrained linear projection with weight matrix $\mathbf{W} \in \mathbb{R}^{d_1 \times d_2}$ and input $\mathbf{X} \in \mathbb{R}^{N \times d_1}$ (a batch of N calibration activations). The layer output is $\mathbf{Z} = \mathbf{X}\mathbf{W} \in \mathbb{R}^{N \times d_2}$. Post-training compression replaces \mathbf{W} by a structured approximation $\tilde{\mathbf{W}}$ that reduces storage and ideally improves inference efficiency.

A common starting point is **weight-space reconstruction**:

$$\tilde{\mathbf{W}}^* = \arg \min_{\tilde{\mathbf{W}} \in \mathcal{C}} \|\mathbf{W} - \tilde{\mathbf{W}}\|_F^2, \quad (1)$$

where \mathcal{C} encodes a chosen structure (e.g., rank- r , sparsity, quantization, or a parametric factorization).

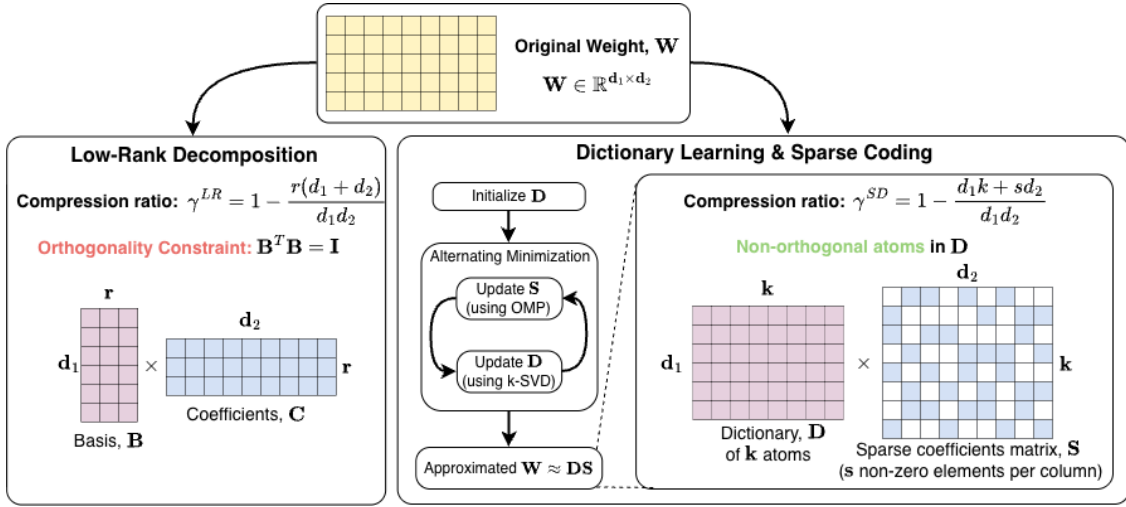


Figure 1: *Left:* low-rank factorization represents \mathbf{W} in a single r -dimensional subspace via two dense factors. *Right:* CoSpaDi represents \mathbf{W} as \mathbf{DS} where \mathbf{D} is a dictionary of k atoms and \mathbf{S} is column-sparse (at most s nonzeros per column), yielding a union-of-subspaces model. Dictionaries may be undercomplete ($k < d_1$), complete ($k = d_1$), or overcomplete ($k > d_1$).

For LLM projections, however, preserving weights is often a weak proxy for preserving model behavior. A more directly relevant goal is **activation-space (functional) reconstruction** on calibration data:

$$\tilde{\mathbf{W}}^* = \arg \min_{\tilde{\mathbf{W}} \in \mathcal{C}} \|\mathbf{X}\mathbf{W} - \mathbf{X}\tilde{\mathbf{W}}\|_F^2. \quad (2)$$

Objective (2) is used (implicitly or explicitly) across many calibration-guided post-training methods, and motivates the activation-aware design of CoSpaDi.

3.2 Truncated SVD as PCA: basis \times coefficients

Low-rank approximation chooses $\mathcal{C} = \{\tilde{\mathbf{W}} : \text{rank}(\tilde{\mathbf{W}}) \leq r\}$ and solves (1):

$$\tilde{\mathbf{W}}^{\text{LR}} = \arg \min_{\text{rank}(\tilde{\mathbf{W}}) \leq r} \|\mathbf{W} - \tilde{\mathbf{W}}\|_F^2. \quad (3)$$

According to the EckartYoungMirsky theorem (Eckart & Young, 1936), the orthogonal projection to the space of r -rank matrices admits an analytical solution. Specifically, if \mathbf{W} admits the singular value decomposition $\mathbf{W} = \mathbf{U}\Sigma\mathbf{V}^\top$, with $\mathbf{U} \in \mathbb{R}^{d_1 \times k}$, $\Sigma \in \mathbb{R}^{k \times k}$ and $\mathbf{V} \in \mathbb{R}^{d_2 \times k}$ with $k = \min(d_1, d_2)$, then the minimizer of Eq. (3) can be expressed as: $\tilde{\mathbf{W}}^{\text{LR}} = \mathbf{U}_r \Sigma_r \mathbf{V}_r^\top$, where $\mathbf{U}_r \in \mathbb{R}^{d_1 \times r}$ contains the first r left singular vectors, $\Sigma_r \in \mathbb{R}^{r \times r}$ holds the top- r singular values, and $\mathbf{V}_r \in \mathbb{R}^{d_2 \times r}$ contains the first r right singular vectors of \mathbf{W} , respectively.

There is a deep connection between this problem and the principal component analysis (PCA) (Bishop & Nasrabadi, 2006). Specifically, consider the weight matrix \mathbf{W} as a collection of d_1 -dimensional vectors $\mathbf{W} = [\mathbf{w}_1, \dots, \mathbf{w}_{d_2}]$, where $\mathbf{w}_j \in \mathbb{R}^{d_1}$, with $j = 1, \dots, d_2$. We seek to approximate each vector \mathbf{w}_j as a linear combination of basis vectors spanning a lower-dimensional subspace of \mathbb{R}^{d_1} . The optimal basis $\mathbf{B} \in \mathbb{R}^{d_1 \times r}$ and coefficients $\mathbf{C} \in \mathbb{R}^{r \times d_2}$ can be found by minimizing the total approximation error:

$$\min_{\mathbf{B}, \mathbf{C}} \|\mathbf{W} - \mathbf{BC}\|_F^2 \quad \text{s.t. } \mathbf{B}^\top \mathbf{B} = \mathbf{I}. \quad (4)$$

The optimum is $\mathbf{B}^* = \mathbf{U}_r$ and $\mathbf{C}^* = \Sigma_r \mathbf{V}_r^\top$ (see Appendix A.1 for the proof). Therefore, truncated SVD realizes a *single shared* r -dimensional subspace: every column \mathbf{w}_j is expressed in the same basis \mathbf{B} via dense coordinates (the j -th column of \mathbf{C}).

Although Eq. (3) minimizes reconstruction error in weight space, several works (e.g., (Chen et al., 2021)) note that LLM projection matrices often lack strong intrinsic low-rank structure, so directly approximating \mathbf{W} can lead to noticeable degradation. A common alternative is to optimize *functional* reconstruction on calibration activations, motivated by the hypothesis that layer inputs lie in a lower-dimensional subspace and that preserving the induced outputs is more relevant than preserving weights in isolation. Concretely, this leads to minimizing $\|\mathbf{XW} - \mathbf{X}\tilde{\mathbf{W}}\|_F^2$ for calibration inputs \mathbf{X} (Chen et al., 2021; Hsu et al., 2022; Yuan et al., 2023; Wang et al., 2025c). In this setting, the optimal low-rank approximation can still be obtained in closed form after applying an activation-derived Gram orthonormalization; we provide the full derivation and solution in Appendix A.2.

3.3 Sparse dictionary learning: union of subspaces

Dictionary learning keeps the “basis times coefficients” form but changes the modeling assumptions. We replace the orthonormal basis \mathbf{B} by a (generally non-orthogonal) dictionary $\mathbf{D} \in \mathbb{R}^{d_1 \times k}$ and enforce *column sparsity* in the coefficient matrix $\mathbf{S} \in \mathbb{R}^{k \times d_2}$:

$$\min_{\mathbf{D}, \mathbf{S}} \|\mathbf{W} - \mathbf{DS}\|_F^2 \quad \text{s.t. } \|\mathbf{s}_j\|_0 \leq s, \quad \forall j, \quad (5)$$

where \mathbf{s}_j is the j -th column of \mathbf{S} , $\|\cdot\|_0$ denotes the ℓ_0 pseudo-norm, and s indicates the sparsity level.

Compared to low-rank factorization, Eq. (5) differs in two crucial ways: (i) coefficients are sparse, so each column activates only s atoms, and (ii) no orthogonality constraint is imposed on \mathbf{D} , allowing more flexible representations. As a result, columns can live in *different* subspaces spanned by different subsets of atoms: \mathbf{W} is represented using a *union of subspaces* model rather than a single shared subspace.

3.4 CoSpaDi: activation-aware sparse dictionary learning for LLM projections

Motivated by the observation that activations, not projection weights, exhibit low-rank structure, we apply dictionary learning to LLM projection matrices under the activation-space objective (2). Concretely, we choose the constraint set $\mathcal{C} = \{\mathbf{DS} : \mathbf{D} \in \mathbb{R}^{d_1 \times k}, \mathbf{S} \in \mathbb{R}^{k \times d_2}, \|\mathbf{s}_j\|_0 \leq s\}$ and solve

$$\min_{\mathbf{D}, \mathbf{S}} \|\mathbf{XW} - \mathbf{XDS}\|_F^2 \quad \text{s.t. } \|\mathbf{s}_j\|_0 \leq s, \quad \forall j. \quad (6)$$

Gram orthonormalization transform. To simplify Eq. (6), consider the Gram matrix $\mathbf{G} := \mathbf{X}^\top \mathbf{X} \in \mathbb{R}^{d_1 \times d_1}$. We compute a *Gram orthonormalization* matrix \mathbf{L} from the (uncentered) second moment \mathbf{G} such that

$$\mathbf{Y} := \mathbf{XL}^{-1} \quad \text{satisfies} \quad \mathbf{Y}^\top \mathbf{Y} = \mathbf{I}, \quad (7)$$

i.e., \mathbf{Y} has orthogonal columns. In practice, \mathbf{L} can be obtained via QR factorization of \mathbf{X} , or from a factorization of \mathbf{G} (e.g., Cholesky when \mathbf{G} is symmetric positive definite, and an SVD/eigendecomposition-based otherwise). Next, we define the transformed variables $\mathbf{W}_L := \mathbf{LW}$ and $\mathbf{D}_L := \mathbf{LD}$. Using the invariance of the Frobenius norm under left multiplication by a column-orthogonal matrix, Eq. (6) reduces to

$$\min_{\mathbf{D}_L, \mathbf{S}} \|\mathbf{W}_L - \mathbf{D}_L \mathbf{S}\|_F^2 \quad \text{s.t. } \|\mathbf{s}_j\|_0 \leq s, \quad \forall j. \quad (8)$$

After solving (8), we map back to the original parameterization:

$$\tilde{\mathbf{W}} = \mathbf{D}_a \mathbf{S}, \quad \mathbf{D}_a = \mathbf{L}^{-1} \mathbf{D}_L. \quad (9)$$

Thus, calibration data enters only through the “whitening” transform \mathbf{L} , while the core optimization reduces to standard sparse dictionary learning on \mathbf{W}_L .

Optimization via alternating minimization. We approximately solve (8) by alternating between sparse coding and dictionary update:

- **Sparse coding.** For each column $\mathbf{w}_{L,j}$ of \mathbf{W}_L , we compute a sparse code \mathbf{s}_j with at most s nonzeros by approximately solving $\min_{\mathbf{s}_j} \|\mathbf{w}_{L,j} - \mathbf{D}_L \mathbf{s}_j\|_2^2$ s.t. $\|\mathbf{s}_j\|_0 \leq s$, using orthogonal matching pursuit (OMP) (Tropp & Gilbert, 2007).
- **Dictionary update.** With sparse supports fixed, we update the dictionary. Two common options are: (i) *MOD* (method of optimal directions), which updates all atoms jointly via a global least-squares step (Engan et al., 1999), and (ii) *K-SVD*, which updates atoms sequentially by solving a rank-1 approximation on a restricted residual (Aharon et al., 2006). Concretely, for atom i let $\Omega_i = \{j : (\mathbf{s}_j)_i \neq 0\}$ be the set of columns using atom i and form the restricted residual $\mathbf{E}_i = (\mathbf{W}_L - \sum_{p \neq i} \mathbf{d}_p \mathbf{s}_{p,:})_{[:, \Omega_i]}$. K-SVD updates \mathbf{d}_i and \mathbf{s}_{i, Ω_i} via the top rank-1 component of \mathbf{E}_i , which can be computed exactly by SVD or approximated with truncated/randomized low-rank routines (Halko et al., 2011) or power iterations (Golub & Van Loan, 2013). In practice, both steps admit efficient implementations, e.g., Batch-OMP for sparse coding and approximate rank-1 updates for K-SVD, substantially reducing runtime and memory overhead (Rubinstein et al., 2008).

Across our ablations, K-SVD with power-iteration rank-1 updates as well as Batch-OMP provides the strongest performance under a reasonable wall-clock budget. The full procedure is summarized in Appendix 1.

3.5 Grouped / shared-dictionary extension

To exploit inter-layer redundancy, we optionally share a dictionary across a group of projections of the same type. Let $\mathcal{G} = \{\ell_1, \dots, \ell_L\}$ be a set of layers with weights $\mathbf{W}_\ell \in \mathbb{R}^{d_1 \times d_2}$. We form a grouped matrix by concatenation

$$\mathbf{W}_\mathcal{G} = [\mathbf{W}_{\ell_1}, \dots, \mathbf{W}_{\ell_L}] \in \mathbb{R}^{d_1 \times (Ld_2)}. \quad (10)$$

To preserve functional fidelity across the group, we stack calibration inputs $\mathbf{X}_\mathcal{G} = [\mathbf{X}_{\ell_1}^\top, \dots, \mathbf{X}_{\ell_L}^\top]^\top \in \mathbb{R}^{(LN) \times d_1}$, compute a Gram orthonormalization matrix \mathbf{L} from $\mathbf{X}_\mathcal{G}$, and solve (8) on $\mathbf{W}_{\mathcal{G},L} = \mathbf{L} \mathbf{W}_\mathcal{G}$ to obtain a shared dictionary and block-structured sparse codes. Each layer is then recovered by slicing the corresponding coefficient block.

This approach, inspired by Basis Sharing (Wang et al., 2025a), reduces memory overhead by amortizing the dictionary cost across multiple layers, while preserving activation fidelity through data-aware calibration. Each layers compressed weights are then recovered by slicing the corresponding coefficient block. Specifically, if $\mathbf{S}_\mathcal{G} \in \mathbb{R}^{k \times (Ld_2)}$ are the learned codes, then the codes for layer ℓ_t are $\mathbf{S}_{\ell_t} = \mathbf{S}_\mathcal{G}[:, (t-1)d_2 : td_2]$.

3.6 Compression ratio

For low-rank factorization with rank r , storing two dense factors costs $r(d_1 + d_2)$ parameters, leading to a compression ratio:

$$\gamma^{\text{LR}} := 1 - \frac{r(d_1 + d_2)}{d_1 d_2}. \quad (11)$$

For CoSpaDi, we store a dense dictionary $\mathbf{D} \in \mathbb{R}^{d_1 \times k}$ and sparse coefficients $\mathbf{S} \in \mathbb{R}^{k \times d_2}$. With s nonzeros per column, the number of stored coefficient values is sd_2 (plus indices/mask; see Appendix A.4 for exact accounting). Thus, we can write

$$\gamma^{\text{SD}} := 1 - \frac{\overbrace{d_1 k}^{\text{dict.}} + \overbrace{sd_2}^{\text{values}} + \overbrace{(kd_2)/16}^{\text{mask}}}{d_1 d_2}. \quad (12)$$

Unlike low-rank compression, γ^{SD} depends on two knobs (k, s) , enabling additional flexibility at a fixed storage budget. We parameterize the trade-off via $\rho := k/s$, which uniquely determines (k, s) at a target γ^{SD} :

$$k = \frac{(1 - \gamma^{\text{SD}}) d_1 d_2}{d_1 + \frac{d_2}{\rho} + \frac{d_2}{16}}, \quad s = \frac{k}{\rho}. \quad (13)$$

3.7 Inference complexity

In terms of computational efficiency, low-rank and dictionary learning exhibit distinct inference-time complexity profiles: the former has a cost of $Nr(d_1 + d_2)$, whereas the latter – when exploiting sparsity and reusing inner products – achieves $Nd_1K_{\text{active}} + Nsd_2$, potentially yielding superior efficiency under favorable sparsity patterns. Although both methods share identical theoretical complexity under matched compression ratios (Appendix A.5), practical inference latency varies significantly due to factors such as the number of active atoms, indexing overhead, and hardware-specific kernel efficiency. Further details regarding complexity derivations are provided in Appendix A.5.

4 Experiments

We evaluate CoSpaDi in two regimes: **per-layer** compression, where each projection matrix is compressed independently, and **grouped (cross-layer)** compression, where a dictionary is shared across a set of layers of the same type. We first present ablations that isolate key design choices (dictionary capacity allocation, data-awareness, packing/quantization, and solver variants), and then report main results for both regimes.

4.1 Experimental Setup

Models and layers. We evaluate per-layer compression on LLaMA-3.2-1B, Qwen-3-0.6B, LLaMA-3-8B, Qwen-3-8B and Qwen-3-14B. For *SVD-LLM* we used the original code-base¹ with only first step on compression without extra finetuning. For grouped compression, we follow the *Basis Sharing*² protocol and report results on LLaMA-2-7B. Unless stated otherwise, we compress all dense linear projections in self-attention (Q/K/V/O) and gated MLP (up/down/gate), while leaving embeddings and the LM head intact.

Calibration data and metrics. For calibration we randomly sample 256 sequences of length 1024 from RefinedWeb (Penedo et al., 2023). We report standard zero-shot accuracy (normalized when available) on a suite of benchmarks (PIQA (Bisk et al., 2020), HellaSwag (Zellers et al., 2019), OpenAI LAMBADA (Paperno et al., 2016), ARC-easy/ARC-challenge (Clark et al., 2018), SciQ (Welbl et al., 2017), Race (Lai et al., 2017), MMLU (Hendrycks et al., 2021)) and perplexity on WikiText (Merity et al., 2017) and OpenAI LAMBADA. We used lm-evaluation-harness 0.4.8 (Gao et al., 2024) to ensure reproducibility.

Compression parameterization. For low-rank baselines, the target compression ratio (CR) uniquely determines the rank r . For CoSpaDi, CR is achieved by choosing the dictionary size k and sparsity s (nonzeros per column), with $\rho := k/s$ controlling how capacity is split between *breadth* (more atoms) and *depth* (more active atoms per column).

Baselines. In the per-layer setting we compare primarily to SVD-LLM (data-aware) (Wang et al., 2025c) and, where relevant, to plain truncated SVD (data-free). We also include comparisons to training-free structured pruning baselines.

We intentionally omit SVD-LLM v2 (Wang et al., 2025b) and Dobi-SVD (Qinsi et al., 2025) from the main baseline set for scope and fairness. Both methods emphasize *dynamic* (layer-wise) compression allocation, which is largely orthogonal to our contribution. Such allocation strategies are not specific to SVD and could be transferred to CoSpaDi by choosing (k_ℓ, s_ℓ) per layer under a global budget. In addition, SVD-LLM v2 does not provide an official implementation, making it difficult to reproduce calibration and allocation details reliably and to apply them consistently in a dictionary-learning setting. Dobi-SVD further departs from our training-free protocol by requiring backpropagation to optimize the allocation. Its reported gains are also coupled to a quantization-specific “remapping” representation that changes the effective storage accounting. In particular, at moderate compression levels (e.g., CR < 0.5), packing two 16-bit values into a single unit can lead to an effective overparameterization relative to standard bf16 storage. For these reasons, we focus

¹<https://github.com/AIoT-MLSys-Lab/SVD-LLM>

²https://github.com/TUDa-HWAI/Basis_Sharing

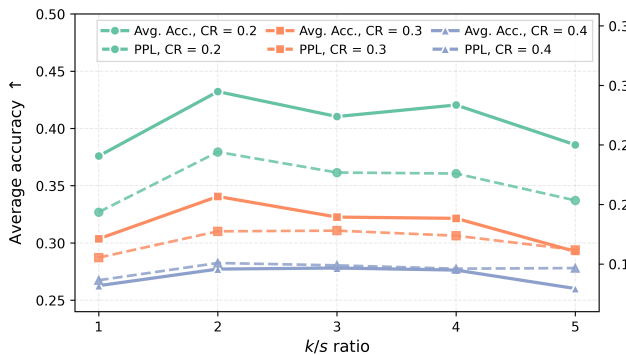


Figure 2: Dual-axis plot showing average accuracy (— solid lines, left axis) and WikiText perplexity (--- dashed lines, right axis, inverted logarithmic scale) as functions of ρ for Llama3.2-1B under three compression levels: 0.2, 0.3 and 0.4.

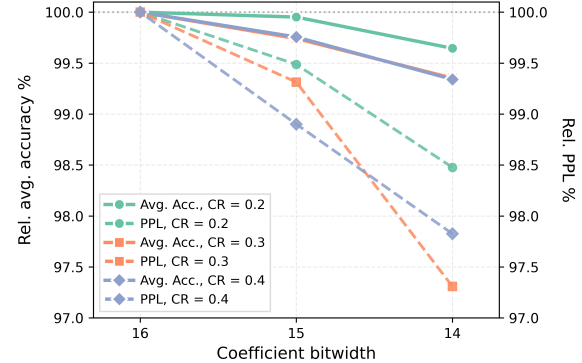


Figure 3: Dual-axis plot showing relative average accuracy (— solid lines, left axis) and relative WikiText perplexity (--- dashed lines, right axis) as functions of S bitwidth for Llama3-8B under three compression levels: 0.2, 0.3 and 0.4.

on reproducible training-free baselines with standard storage conventions, and view dynamic allocation and quantization-specific representations as complementary extensions.

4.2 Ablation Studies

4.2.1 Capacity Allocation: the k/s Ratio

At a fixed compression ratio (CR), CoSpaDi admits a family of factorizations parameterized by $\rho := k/s$. Smaller ρ increases per-column expressiveness (larger s) but reduces the dictionary size k ; larger ρ increases k but restricts each column to fewer active atoms. We perform a coarse sweep over $\rho \in [1; 5]$. Figure 2 (LLaMA-3.2-1B) shows that $\rho = 2$ consistently provides the best trade-off across all considered CRs in terms of both average accuracy and perplexity. We therefore fix $\rho = 2$ in all subsequent experiments for simplicity and comparability across models.

Notably, $\rho = 1$ corresponds to the degenerate regime $k = s$, where each column may activate all atoms. In this case, the sparsity constraint becomes inactive and CoSpaDi reduces to a dense two-factor approximation, closely mirroring the “basis times coefficients” view underlying truncated SVD/PCA. This emphasizes that CoSpaDi can be seen as a strict generalization: choosing $\rho > 1$ enforces sparsity and yields a union-of-subspaces model.

4.2.2 Data-Free vs. Data-Aware Compression

A core motivation for dictionary learning is that its union-of-subspaces form can be more expressive than a single low-dimensional subspace *regardless of whether calibration is used*. We therefore compare: (i) **data-free** truncated SVD vs. CoSpaDi † (dictionary learning in weight space, without whitening), and (ii) **data-aware** SVD-LLM vs. CoSpaDi (activation-aware via whitening). Table 2 summarizes results on LLaMA-3.2-1B across CR 0.2–0.4. In both regimes, the dictionary-based factorization is consistently stronger than the corresponding low-rank baseline, and activation-aware CoSpaDi yields the best overall trade-off.

4.2.3 Dictionary Learning Solver Variants: Exact K-SVD vs. Power-K-SVD vs. MOD

The main bottleneck in the alternating minimization process is the dictionary update using K-SVD as it updates a single atom at a time. To reduce its computational cost we investigate the usage of truncated PCA and power iterations for solving rank-1 problems as well as the well-known Method of Optimal Directions (MOD) which updates in a single step the entire dictionary instead of individual atoms sequentially.

Table 1: SDL-based methods comparison vs low-rank counterparts in data-free and data-aware scenarios on Llama3.2-1B at different compression ratios (CR). We denote CoSpaDi † as the proposed method without using calibration data. Best results are provided in **bold**.

Method	Data-Aware	CR	Accuracy \uparrow								Perplexity \downarrow		
			PIQA	Hella Swag	LAMBADA	ARC-e	ARC-c	SciQ	Race	MMLU	Avg.	Wiki Text	LAMBADA
Llama3.2 1B	—	—	74.5	63.7	63.0	60.5	36.2	88.3	37.8	37.0	57.6	11.6E+00	5.7E+00
SVD	✗	—	52.0	25.7	0.0	24.7	22.1	20.0	21.4	25.4	23.9	2.9E+06	4.6E+06
CoSpaDi †	✗	—	51.7	26.4	0.0	25.4	25.3	21.0	21.8	24.1	24.5	3.3E+05	2.2E+06
SVD-LLM	✓	0.2	62.1	36.4	24.4	36.0	25.1	64.9	29.0	23.0	37.6	1.7E+02	1.7E+02
CoSpaDi	✓	—	66.1	42.9	38.4	39.9	26.0	71.6	31.7	24.8	42.7	6.4E+01	3.5E+01
SVD	✗	—	52.3	25.6	0.0	24.2	23.5	19.5	21.9	27.0	24.3	1.1E+06	3.9E+06
CoSpaDi †	✗	—	50.5	26.3	0.0	24.5	26.1	21.8	21.5	25.5	24.5	2.1E+05	4.3E+06
SVD-LLM	✓	0.3	55.7	30.1	9.1	30.5	21.5	45.9	25.8	23.2	30.2	5.9E+02	2.5E+03
CoSpaDi	✓	—	56.9	32.4	18.2	31.9	22.1	56.7	28.0	23.1	33.7	2.9E+02	6.6E+02
SVD	✗	—	52.8	25.9	0.0	23.9	21.3	19.9	22.2	26.9	24.1	1.2E+06	4.2E+06
CoSpaDi †	✗	—	51.0	26.3	0.0	25.5	26.9	21.3	21.2	25.5	24.7	3.1E+06	3.7E+07
SVD-LLM	✓	0.4	51.8	27.3	1.3	26.9	22.9	32.3	24.4	23.0	26.2	1.6E+03	3.3E+04
CoSpaDi	✓	—	53.5	28.2	3.8	27.8	23.0	36.9	24.0	23.1	27.5	8.0E+02	9.2E+03

Table 2 reports both quality (Avg. accuracy, WikiText perplexity) and **wall-clock compression time** at a representative 0.2 CR on LLaMA-3.2-1B. Wall-clock is measured for compressing all targeted projection matrices with identical hardware, batching, and stopping criteria. This comparison isolates the practical speed-quality trade-off of the solver choice while keeping the factorization form (k, s) fixed. For our further experiments we utilized K-SVD using power-iterations as it achieves good performance at a reasonable wall-clock time for compression. We provide a more thorough ablation study on the number of power iterations and of the alternating steps in Appendix A.7

Table 2: Solver comparison for dictionary update on LLaMA-3.2-1B at 0.2 compression ratio (CR) and fixed $\rho = 2, 60$ alternating minimization iterations. We report accuracies, perplexity as well as wall-clock compression time in minutes using a single A100. Best results are highlighted with **bold**.

Method	Wall-clock time	Accuracy \uparrow								Perplexity \downarrow		
		PIQA	Hella Swag	LAMBADA	ARC-e	ARC-c	SciQ	Race	MMLU	Avg.	Wiki Text	LAMBADA
Llama3.2 1B	—	74.5	63.7	63.0	60.5	36.2	88.3	37.8	37.0	57.6	11.6E+00	5.7E+00
MOD	222.2	62.9	39.7	30.4	36.3	25.7	67.6	27.9	23.0	39.2	1.1E+02	8.7E+01
K-SVD (PCA)	902.1	64.4	39.9	33.7	40.5	25.9	72.3	31.6	24.4	41.6	9.6E+01	6.2E+01
K-SVD (power)	646.8	75.2	66.5	73.8	66.5	41.6	89.5	38.2	42.8	61.8	2.0E+01	4.3E+00

4.2.4 Quantizing Coefficients and Removing the Mask Term

Sparse factorization introduces metadata overhead for storing nonzero locations. Our default implementation uses a packed binary mask (one bit per entry) plus bf16 values for the sd_2 nonzeros. We additionally study **post-training coefficient quantization** by truncating bf16 mantissa bits. Plots on Figure 3 shows that truncating 2 mantissa bits yields negligible degradation across tested CRs.

Beyond robustness, coefficient quantization enables a *simplified storage accounting* in which locations can be treated as fixed by construction (e.g., using a deterministic pattern per column or a reproducible pseudo-random seed), removing the explicit mask term from the compression ratio. Under this view, the effective storage becomes

$$\hat{\gamma}^{\text{SD}} = 1 - \frac{d_1 k + sd_2}{d_1 d_2}. \quad (14)$$

Unless stated otherwise, we evaluate CoSpaDi with bf16 dictionaries and truncated (14-bit) coefficients, thus providing CR according to Equation 14.

4.3 Main Results

4.3.1 Per-Layer Compression

We first compress each projection matrix independently and compare CoSpaDi to SVD-LLM over a range of CRs. Figure 4 summarizes the accuracy–compression and perplexity–compression curves for small models (LLaMA-3.2-1B and Qwen-3-0.6B). For larger models, Table 3 reports results on LLaMA-3-8B, Qwen-3-8B and Qwen-3-14B at CR 0.2–0.4. Across model families and budgets, CoSpaDi consistently improves both average benchmark accuracy and perplexity at matched CR, indicating that the union-of-subspaces factorization better preserves task-relevant directions than a single low-rank basis. We provide additional benchmarks in the Appendix A.6.

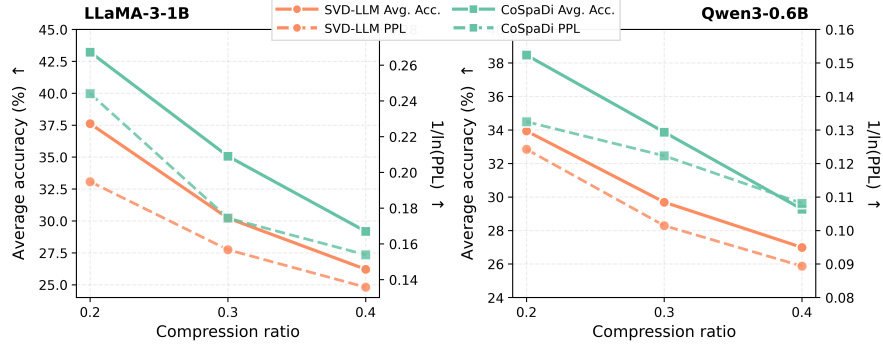


Figure 4: Average benchmark accuracy and WikiText perplexity for LLaMA-3.2-1B and Qwen-3 0.6B using SVD-LLM and CoSpaDi with respect to compression ratio.

Table 3: Performance comparison of CoSpaDi vs sota SVD-LLM on Llama3-8B, Qwen3-8B and Qwen3-14B at different compression levels on different benchmarks. Best results are highlighted with **bold**.

Method	CR	Accuracy↑									Perplexity↓	
		PIQA	Hella Swag	LAMBADA	ARC-e	ARC-c	SciQ	Race	MMLU	Avg.	Wiki Text	LAMBADA
LLama3 8B	–	80.7	79.1	75.6	77.7	53.5	93.9	40.3	62.2	70.4	7.3E+00	3.1E+00
SVD-LLM	0.2	71.1	58.4	59.3	55.5	34.0	86.4	35.5	32.6	54.1	4.1E+01	1.1E+01
CoSpaDi		75.2	66.5	73.8	66.5	41.6	89.5	38.2	42.8	61.8	2.0E+01	4.3E+00
SVD-LLM	0.3	65.8	46.4	38.1	41.9	27.7	70.0	31.8	27.2	43.6	1.5E+02	6.1E+01
CoSpaDi		70.5	56.2	61.3	54.2	33.5	85.7	36.2	32.2	53.7	4.5E+01	9.2E+00
SVD-LLM	0.4	60.3	34.5	11.4	32.4	24.5	44.2	25.7	23.1	32.0	5.5E+02	1.3E+03
CoSpaDi		63.7	41.4	30.3	39.1	26.6	68.5	30.5	25.4	40.7	1.8E+02	1.2E+02
Qwen3 8B	–	77.7	74.9	64.1	80.7	56.7	95.7	40.9	73.0	70.5	1.2E+01	4.6E+00
SVD-LLM	0.2	73.8	63.9	62.2	68.7	45.7	90.1	40.5	54.7	62.5	2.1E+01	6.4E+00
CoSpaDi		76.5	68.0	65.6	72.2	48.9	93.2	40.7	60.8	65.7	1.8E+01	4.9E+00
SVD-LLM	0.3	70.4	55.2	53.8	59.3	37.1	87.2	38.4	44.8	55.8	2.7E+01	1.1E+01
CoSpaDi		72.4	60.5	62.6	63.9	41.2	88.4	39.5	51.3	59.97	2.3E+01	6.3E+00
SVD-LLM	0.4	66.3	44.6	37.9	45.0	28.1	77.3	35.3	29.1	45.4	4.3E+01	3.6E+01
CoSpaDi		68.9	49.0	49.9	49.4	29.9	82.0	36.8	36.6	50.3	3.6E+01	1.5E+01
Qwen3 14B	–	79.9	78.9	67.9	82.8	60.2	96.5	43.3	77.2	73.3	1.1E+01	3.7E+00
SVD-LLM	0.2	76.2	67.6	69.1	69.8	46.8	91.0	42.9	62.5	65.8	1.8E+01	4.1E+00
CoSpaDi		77.3	71.7	72.0	73.3	51.3	91.9	43.1	65.8	68.3	1.6E+01	3.4E+00
SVD-LLM	0.3	72.0	59.7	61.5	62.6	39.3	88.9	41.5	52.0	59.7	2.3E+01	6.5E+00
CoSpaDi		74.6	64.2	69.0	65.3	43.6	90.7	42.5	58.0	63.5	2.0E+01	4.2E+00
SVD-LLM	0.4	67.4	48.7	46.0	48.5	30.7	80.6	36.7	36.8	49.4	3.5E+01	1.8E+01
CoSpaDi		69.5	52.3	57.3	53.2	33.0	84.4	37.5	43.6	53.9	3.3E+01	8.7E+00

4.3.2 Comparison with Pruning

We additionally compare CoSpaDi to recent *structured* pruning approaches on the same models and compression ratios. Specifically, we evaluate against ReplaceMe (Shopkhoev et al., 2025) and LLM-Pruner (Ma et al., 2023), which are representative state-of-the-art methods that reduce parameters by removing or replacing structured components (e.g., blocks/layers) rather than individual weights. Results are reported in Table 4.

We do not include *unstructured* pruning baselines in this comparison because their practical memory savings depend on sparse storage formats and hardware support; at moderate sparsity levels (e.g., $\approx 50\%$), the overhead of storing indices and irregular access patterns often diminishes or eliminates effective compression and speedups in standard dense inference pipelines.

Table 4: Comparison of the proposed CoSpaDi method with state-of-the-art structured pruning methods ReplaceMe Shopkhoev et al. (2025) and LLM-Pruner Ma et al. (2023) on Llama3 8B under different compression ratios. We report accuracy on different benchmarks as well as its average and perplexity. Best results are highlighted with **bold**

Method	CR	Accuracy \uparrow								Perplexity \downarrow		
		PIQA	Hella Swag	LAMBADA	ARC-e	ARC-c	SciQ	Race	MMLU	Avg.	Wiki Text	LAMBADA
Llama3 8B		80.7	79.1	75.6	77.7	53.5	93.9	40.3	62.2	70.4	7.3E+00	3.1E+00
ReplaceMe	0.22	73.1	65.7	42.1	65.9	43.7	86.4	35.4	51.7	58.0	3.4E+01	2.0E+01
LLM-Pruner	0.2	75.5	67.5	51.0	62.1	36.6	87.8	35.1	25.0	55.1	1.6E+01	1.1E+01
CoSpaDi		75.2	66.5	73.8	66.5	41.6	89.5	38.2	42.8	61.8	2.0E+01	4.3E+00
ReplaceMe	0.31	66.6	53.8	24.0	50.7	37.9	77.3	34.0	30.6	46.9	6.7E+01	1.3E+02
LLM-Pruner	0.3	67.3	45.1	20.9	45.4	28.8	63.4	30.1	22.9	40.5	3.8E+01	2.2E+02
CoSpaDi		70.5	56.2	61.3	54.2	33.5	85.7	36.2	32.2	53.7	4.5E+01	9.2E+00
ReplaceMe	0.41	61.7	44.3	9.8	37.4	27.5	60.4	31.6	26.4	37.4	2.3E+02	1.8E+03
LLM-Pruner	0.4	50.3	25.8	1.5	26.4	25.8	28.1	21.8	23.2	25.4	∞	5.7E+05
CoSpaDi		63.7	41.4	30.3	39.1	26.6	68.5	30.5	25.4	40.7	1.8E+02	1.2E+02

4.3.3 Grouped (Cross-Layer) Dictionary Sharing

Next, we evaluate grouped compression where a single dictionary is shared across multiple layers of the same projection type. For a fair and controlled comparison, we adopt the *exact* layer grouping and evaluation protocol of Basis Sharing, i.e., we share parameters across the same layer sets and report results under the same compression budgets. Table 5 reports results on LLaMA-2-7B across CR 0.2–0.4. We additionally included per-layer counterparts to show the benefits of grouping strategy and exploiting inter-layer redundancies. At all budgets, CoSpaDi substantially outperforms Basis Sharing as well as per-layer baselines, suggesting that cross-layer sharing is most effective when paired with sparse codes that allow each column (and each layer) to select its own subset of atoms. We note that CoSpaDi does not rely on this particular grouping and could benefit from more adaptive sharing strategies (e.g., data-driven grouping or partially shared dictionaries), which we leave for future work.

5 Open Issues and Future Work

Solver efficiency and scalability. CoSpaDi uses alternating minimization with OMP for sparse coding and K-SVD-style sequential atom updates. This is simple and effective but can be expensive due to repeated sparse coding and per-atom updates, especially for large matrices and aggressive compression. Faster variants (e.g., more parallel updates, better batching, or alternative sparse coding) are promising; our ablations already show that approximate rank-1 updates (e.g., power iterations) offer a favorable accuracy–time trade-off.

Hyperparameter selection and dynamic budget allocation. We parameterize CoSpaDi via (k, s) and $\rho = k/s$, but fix ρ and use uniform budgets for simplicity. Prior low-rank work shows that layer-/type-wise

Table 5: Performance comparison of CoSpaDi vs Basis Sharing (Wang et al., 2025a) and per-layer counterparts on Llama2-7B under different compression levels on various benchmarks. Best results are highlighted with **bold**.

Method	CR	Accuracy↑								Perplexity↓			
		PIQA	Hella Swag	LAMBADA	ARC-e	ARC-c	SciQ	Race	MMLU	Avg.	Wiki	Text	LAMBADA
Llama2 7B	–	78.0	57.1	73.7	76.1	43.3	93.9	39.2	40.9	62.8	8.7	3.4	
SVD-LLM		73.3	60.4	64.0	55.1	32.3	79.7	36.6	25.5	53.4	20.2	6.3	
CoSpaDi (per-layer)	0.2	74.3	64.8	70.2	61.6	35.3	85.8	39.0	28.2	57.4	15.8	4.5	
Basis Sharing		70.1	43.4	63.0	66.5	33.7	91.0	34.9	24.8	53.4	15.2	7.2	
CoSpaDi (grouped)		74.6	66.3	71.3	67.4	39.3	88.8	38.3	27.2	59.2	11.7	4.3	
SVD-LLM		68.4	52.2	51.5	46.8	27.8	75.9	34.7	23.5	47.6	34.0	13.5	
CoSpaDi (per-layer)	0.3	71.2	57.4	62.7	53.5	30.6	81.6	36.8	26.9	52.6	23.6	6.9	
Basis Sharing		65.6	37.6	53.5	58.8	27.3	86.8	32.6	23.2	48.2	22.2	13.6	
CoSpaDi (grouped)		70.8	58.5	64.5	61.9	34.3	87.6	35.9	24.0	54.7	15.4	6.3	
SVD-LLM		63.2	42.7	33.1	37.7	24.6	70.2	32.2	23.0	40.8	86.5	67.1	
CoSpaDi (per-layer)	0.4	66.2	48.4	47.2	44.3	26.2	76.7	33.4	23.4	45.7	49.2	20.9	
Basis Sharing		60.6	33.1	41.1	49.5	23.6	83.0	29.7	23.1	42.95	39.5	37.7	
CoSpaDi (grouped)		64.3	48.0	51.8	52.3	29.9	81.5	33.2	23.0	48.0	25.2	14.6	

sensitivity can improve quality at a fixed global budget. Adapting dynamic allocation to dictionary learning—e.g., choosing (k_ℓ, s_ℓ) per layer, projection type, or group based on functional sensitivity—is a promising direction.

Grouped sharing design choices. Grouped performance depends on how layers are clustered and which projections share a dictionary. We follow a simple grouping aligned with prior cross-layer sharing, while more adaptive grouping based on activation/weight similarity could yield additional gains.

Practical speedups depend on kernel support. CoSpaDi yields structured sparsity exploitable by sparse–dense computation, but end-to-end speedups depend on sparse kernel efficiency, indexing overhead, and reuse of intermediate products. Encouragingly, recent work reports strong acceleration for dense–sparse matmul even at modest sparsity, narrowing the gap between parameter reduction and wall-clock benefits (Macko & Boa, 2025). Realizing consistent speedups will require integration into optimized inference runtimes and hardware-aware kernels for the resulting computation patterns.

Beyond the current instantiation. Our goal is to introduce activation-aware sparse dictionary learning as a new post-training compression paradigm beyond single-subspace (low-rank) approximations. Accordingly, we use a direct optimization pipeline. Many advances from low-rank compression–richer calibration objectives, better sensitivity measures, and refined allocation strategies—could be transferred to this setting without changing the core factorization.

6 Conclusion

We presented CoSpaDi, a training-free LLM compression framework based on sparse dictionary learning. CoSpaDi factorizes projection matrices into a dense dictionary and column-sparse codes, moving from a single shared low-dimensional subspace to a union-of-subspaces representation. Using a small calibration set, an activation-derived Gram orthonormalization converts functional output reconstruction into a tractable dictionary learning objective solved by alternating sparse coding and dictionary updates.

Across multiple Llama and Qwen models, CoSpaDi improves the accuracy–compression and perplexity–compression trade-offs over strong SVD-based baselines in both per-layer and grouped (shared-dictionary) settings at 20–40% compression ratios, and composes naturally with post-training coefficient quantization. More broadly, our results highlight dictionary learning as a flexible paradigm for post-training compression and suggest that many advances from low-rank methods (e.g., dynamic allocation and improved calibration objectives) can be transferred to this richer factorization family.

References

Josh Achiam, Steven Adler, Sandhini Agarwal, Lama Ahmad, Ilge Akkaya, Florencia Leoni Aleman, Diogo Almeida, Janko Altenschmidt, Sam Altman, Shyamal Anadkat, et al. Gpt-4 technical report. *arXiv preprint arXiv:2303.08774*, 2023.

Michal Aharon, Michael Elad, and Alfred Bruckstein. K-svd: An algorithm for designing overcomplete dictionaries for sparse representation. *IEEE Transactions on signal processing*, 54(11):4311–4322, 2006.

Rohan Anil, Andrew M Dai, Orhan Firat, Melvin Johnson, Dmitry Lepikhin, Alexandre Passos, Siamak Shakeri, Emanuel Taropa, Paige Bailey, Zhifeng Chen, et al. Palm 2 technical report. *arXiv preprint arXiv:2305.10403*, 2023.

Saleh Ashkboos, Amirkeivan Mohtashami, Maximilian L Croci, Bo Li, Pashmina Cameron, Martin Jaggi, Dan Alistarh, Torsten Hoefer, and James Hensman. Quarot: Outlier-free 4-bit inference in rotated llms. *Advances in Neural Information Processing Systems*, 37:100213–100240, 2024.

Christopher M Bishop and Nasser M Nasrabadi. *Pattern recognition and machine learning*, volume 4. Springer, 2006.

Yonatan Bisk, Rowan Zellers, Jianfeng Gao, Yejin Choi, et al. Piqa: Reasoning about physical commonsense in natural language. In *Proceedings of the AAAI conference on artificial intelligence*, volume 34, pp. 7432–7439, 2020.

Tom Brown, Benjamin Mann, Nick Ryder, Melanie Subbiah, Jared D Kaplan, Prafulla Dhariwal, Arvind Neelakantan, Pranav Shyam, Girish Sastry, Amanda Askell, et al. Language models are few-shot learners. *Advances in neural information processing systems*, 33:1877–1901, 2020.

Patrick Chen, Si Si, Yang Li, Ciprian Chelba, and Cho-Jui Hsieh. Groupreduce: Block-wise low-rank approximation for neural language model shrinking. *Advances in Neural Information Processing Systems*, 31, 2018.

Patrick Chen, Hsiang-Fu Yu, Inderjit Dhillon, and Cho-Jui Hsieh. Drone: Data-aware low-rank compression for large nlp models. *Advances in neural information processing systems*, 34:29321–29334, 2021.

Peter Clark, Isaac Cowhey, Oren Etzioni, Tushar Khot, Ashish Sabharwal, Carissa Schoenick, and Oyvind Tafjord. Think you have solved question answering? try arc, the ai2 reasoning challenge, 2018.

Emily L Denton, Wojciech Zaremba, Joan Bruna, Yann LeCun, and Rob Fergus. Exploiting linear structure within convolutional networks for efficient evaluation. *Advances in neural information processing systems*, 27, 2014.

Tim Dettmers, Mike Lewis, Younes Belkada, and Luke Zettlemoyer. Gpt3. int8 (): 8-bit matrix multiplication for transformers at scale. *Advances in neural information processing systems*, 35:30318–30332, 2022.

Tim Dettmers, Ruslan A. Svirschevski, Vage Egiazarian, Denis Kuznedelev, Elias Frantar, Saleh Ashkboos, Alexander Borzunov, Torsten Hoefer, and Dan Alistarh. SpQR: A sparse-quantized representation for near-lossless LLM weight compression. In *The Twelfth International Conference on Learning Representations*, 2024. URL <https://openreview.net/forum?id=Q1u25ahSuy>.

Jacob Devlin, Ming-Wei Chang, Kenton Lee, and Kristina Toutanova. Bert: Pre-training of deep bidirectional transformers for language understanding. In *Proceedings of the 2019 conference of the North American chapter of the association for computational linguistics: human language technologies, volume 1 (long and short papers)*, pp. 4171–4186, 2019.

Carl Eckart and Gale Young. The approximation of one matrix by another of lower rank. *Psychometrika*, 1(3):211–218, 1936.

Michael Elad. *Sparse and redundant representations: from theory to applications in signal and image processing*. Springer Science & Business Media, 2010.

Kjersti Engan, Sven Ole Aase, and John Hakon Husoy. Frame based signal compression using method of optimal directions (mod). In *1999 IEEE International symposium on circuits and systems (ISCAS)*, volume 4, pp. 1–4. IEEE, 1999.

Ky Fan. On a theorem of Weyl concerning eigenvalues of linear transformations I. *Proceedings of the National Academy of Sciences of the United States of America*, 35(11):652–655, 1949.

Jonathan Frankle and Michael Carbin. The lottery ticket hypothesis: Finding sparse, trainable neural networks. In *International Conference on Learning Representations*, 2019. URL <https://openreview.net/forum?id=rJ1-b3RcF7>.

Elias Frantar and Dan Alistarh. Sparsegpt: Massive language models can be accurately pruned in one-shot. In *International conference on machine learning*, pp. 10323–10337. PMLR, 2023.

Elias Frantar, Saleh Ashkboos, Torsten Hoefer, and Dan Alistarh. Gptq: Accurate post-training quantization for generative pre-trained transformers, 2023a. URL <https://arxiv.org/abs/2210.17323>.

Elias Frantar, Saleh Ashkboos, Torsten Hoefer, and Dan Alistarh. OPTQ: Accurate quantization for generative pre-trained transformers. In *The Eleventh International Conference on Learning Representations*, 2023b. URL <https://openreview.net/forum?id=tcbBPnfwxS>.

Leo Gao, Jonathan Tow, Baber Abbasi, Stella Biderman, Sid Black, Anthony DiPofi, Charles Foster, Laurence Golding, Jeffrey Hsu, Alain Le Noac'h, Haonan Li, Kyle McDonell, Niklas Muennighoff, Chris Ociepa, Jason Phang, Laria Reynolds, Hailey Schoelkopf, Aviya Skowron, Lintang Sutawika, Eric Tang, Anish Thite, Ben Wang, Kevin Wang, and Andy Zou. The language model evaluation harness, 07 2024. URL <https://zenodo.org/records/12608602>.

Gene H. Golub and Charles F. Van Loan. *Matrix Computations*. Johns Hopkins University Press, 4 edition, 2013.

Karol Gregor and Yann LeCun. Learning fast approximations of sparse coding. In *Proceedings of the 27th international conference on international conference on machine learning*, pp. 399–406, 2010.

Nathan Halko, Per-Gunnar Martinsson, and Joel A. Tropp. Finding structure with randomness: Probabilistic algorithms for constructing approximate matrix decompositions. *SIAM Review*, 53(2):217–288, 2011.

Song Han, Huizi Mao, and William J. Dally. Deep compression: Compressing deep neural networks with pruning, trained quantization and huffman coding. *arXiv preprint arXiv:1510.00149*, 2015.

Dan Hendrycks, Collin Burns, Steven Basart, Andy Zou, Mantas Mazeika, Dawn Song, and Jacob Steinhardt. Measuring massive multitask language understanding. *Proceedings of the International Conference on Learning Representations (ICLR)*, 2021.

Geoffrey Hinton, Oriol Vinyals, and Jeff Dean. Distilling the knowledge in a neural network. *arXiv preprint arXiv:1503.02531*, 2015.

Yen-Chang Hsu, Ting Hua, Sungen Chang, Qian Lou, Yilin Shen, and Hongxia Jin. Language model compression with weighted low-rank factorization. In *International Conference on Learning Representations*, 2022. URL <https://openreview.net/forum?id=uPv9Y3gmAI5>.

Junhyuck Kim, Jongho Park, Jaewoong Cho, and Dimitris Papailiopoulos. Lexico: Extreme KV cache compression via sparse coding over universal dictionaries. In *Forty-second International Conference on Machine Learning*, 2025. URL <https://openreview.net/forum?id=Yh9vx1xnjA>.

Guokun Lai, Qizhe Xie, Hanxiao Liu, Yiming Yang, and Eduard Hovy. RACE: Large-scale ReADING comprehension dataset from examinations. In Martha Palmer, Rebecca Hwa, and Sebastian Riedel (eds.), *Proceedings of the 2017 Conference on Empirical Methods in Natural Language Processing*, pp. 785–794, Copenhagen, Denmark, September 2017. Association for Computational Linguistics. doi: 10.18653/v1/D17-1082. URL <https://aclanthology.org/D17-1082/>.

Ji Lin, Jiaming Tang, Haotian Tang, Shang Yang, Wei-Ming Chen, Wei-Chen Wang, Guangxuan Xiao, Xingyu Dang, Chuang Gan, and Song Han. Awq: Activation-aware weight quantization for on-device llm compression and acceleration. *Proceedings of machine learning and systems*, 6:87–100, 2024.

Xindian Ma, Peng Zhang, Shuai Zhang, Nan Duan, Yuexian Hou, Ming Zhou, and Dawei Song. A tensorized transformer for language modeling. *Advances in neural information processing systems*, 32, 2019.

Xinyin Ma, Gongfan Fang, and Xinchao Wang. Llm-pruner: On the structural pruning of large language models. *Advances in neural information processing systems*, 36:21702–21720, 2023.

Vladimír Macko and Vladimír Boa. Macko: Sparse matrix-vector multiplication for low sparsity, 2025. URL <https://arxiv.org/abs/2511.13061>.

Julien Mairal, Francis Bach, Jean Ponce, and Guillermo Sapiro. Online dictionary learning for sparse coding. In *Proceedings of the 26th annual international conference on machine learning*, pp. 689–696, 2009.

Stephen Merity, Caiming Xiong, James Bradbury, and Richard Socher. Pointer sentinel mixture models. In *International Conference on Learning Representations*, 2017. URL <https://openreview.net/forum?id=Byj72udxe>.

Asit Mishra, Jorge Albericio Latorre, Jeff Pool, Darko Stosic, Dusan Stosic, Ganesh Venkatesh, Chong Yu, and Paulius Micikevicius. Accelerating sparse deep neural networks. *arXiv preprint arXiv:2104.08378*, 2021.

NVIDIA. Nvidia a100 tensor core gpu architecture. Technical report, NVIDIA, 2020. NVIDIA Ampere Architecture Whitepaper.

Denis Paperno, Germán Kruszewski, Angeliki Lazaridou, Ngoc-Quan Pham, Raffaella Bernardi, Sandro Pezzelle, Marco Baroni, Gemma Boleda, and Raquel Fernández. The lambada dataset: Word prediction requiring a broad discourse context. In *Proceedings of the 54th annual meeting of the association for computational linguistics (volume 1: Long papers)*, pp. 1525–1534, 2016.

Guilherme Penedo, Quentin Malartic, Daniel Hesslow, Ruxandra Cojocaru, Hamza Alobeidli, Alessandro Cappelli, Baptiste Pannier, Ebtesam Almazrouei, and Julien Launay. The refinedweb dataset for falcon LLM: Outperforming curated corpora with web data only. In *Thirty-seventh Conference on Neural Information Processing Systems Datasets and Benchmarks Track*, 2023. URL <https://openreview.net/forum?id=kM5eGcdCzq>.

Wang Qinsi, Jinghan Ke, Masayoshi Tomizuka, Kurt Keutzer, and Chenfeng Xu. Dobi-SVD: Differentiable SVD for LLM compression and some new perspectives. In *The Thirteenth International Conference on Learning Representations*, 2025. URL <https://openreview.net/forum?id=kws76i5XB8>.

Ron Rubinstein, Michael Zibulevsky, and Michael Elad. Efficient implementation of the k-svd algorithm using batch orthogonal matching pursuit. *Cs Technion*, 40(8):1–15, 2008.

Dmitriy Shopkhoev, Ammar Ali, Magauiya Zhussip, Valentin Malykh, Stamatios Lefkimiatis, Nikos Kondakis, and Sergey Zagoruyko. Replaceme: Network simplification via depth pruning and transformer block linearization. In *The Thirty-ninth Annual Conference on Neural Information Processing Systems*, 2025. URL <https://openreview.net/forum?id=zEj1FSYCRn>.

Mingjie Sun, Zhuang Liu, Anna Bair, and J Zico Kolter. A simple and effective pruning approach for large language models. In *The Twelfth International Conference on Learning Representations*, 2024. URL <https://openreview.net/forum?id=PxoFut3dWW>.

Hugo Touvron, Thibaut Lavril, Gautier Izacard, Xavier Martinet, Marie-Anne Lachaux, Timothée Lacroix, Baptiste Rozière, Naman Goyal, Eric Hambro, Faisal Azhar, et al. Llama: Open and efficient foundation language models. *arXiv preprint arXiv:2302.13971*, 2023.

Joel A. Tropp and Anna C. Gilbert. Signal recovery from random measurements via orthogonal matching pursuit. *IEEE Transactions on Information Theory*, 53(12):4655–4666, 2007. doi: 10.1109/TIT.2007.909108.

Ashish Vaswani, Noam Shazeer, Niki Parmar, Jakob Uszkoreit, Llion Jones, Aidan N Gomez, Łukasz Kaiser, and Illia Polosukhin. Attention is all you need. *Advances in neural information processing systems*, 30, 2017.

Jingcun Wang, Yu-Guang Chen, Ing-Chao Lin, Bing Li, and Grace Li Zhang. Basis sharing: Cross-layer parameter sharing for large language model compression. In *The Thirteenth International Conference on Learning Representations*, 2025a. URL <https://openreview.net/forum?id=gp32jvUquq>.

Xin Wang, Samiul Alam, Zhongwei Wan, Hui Shen, and Mi Zhang. Svd-llm v2: Optimizing singular value truncation for large language model compression. *arXiv preprint arXiv:2503.12340*, 2025b.

Xin Wang, Yu Zheng, Zhongwei Wan, and Mi Zhang. SVD-LLM: Truncation-aware singular value decomposition for large language model compression. In *The Thirteenth International Conference on Learning Representations*, 2025c. URL <https://openreview.net/forum?id=LNYIUouhdt>.

Ziheng Wang. Sparsert: Accelerating unstructured sparsity on gpus for deep learning inference. In *Proceedings of the ACM international conference on parallel architectures and compilation techniques*, pp. 31–42, 2020.

Johannes Welbl, Nelson F. Liu, and Matt Gardner. Crowdsourcing multiple choice science questions. In Leon Derczynski, Wei Xu, Alan Ritter, and Tim Baldwin (eds.), *Proceedings of the 3rd Workshop on Noisy User-generated Text*, pp. 94–106, Copenhagen, Denmark, September 2017. Association for Computational Linguistics. doi: 10.18653/v1/W17-4413. URL <https://aclanthology.org/W17-4413/>.

Guangxuan Xiao, Ji Lin, Mickael Seznec, Hao Wu, Julien Demouth, and Song Han. Smoothquant: Accurate and efficient post-training quantization for large language models. In *International conference on machine learning*, pp. 38087–38099. PMLR, 2023.

Zhihang Yuan, Yuzhang Shang, Yue Song, Dawei Yang, Qiang Wu, Yan Yan, and Guangyu Sun. Asvd: Activation-aware singular value decomposition for compressing large language models. *arXiv preprint arXiv:2312.05821*, 2023.

Rowan Zellers, Ari Holtzman, Yonatan Bisk, Ali Farhadi, and Yejin Choi. Hellaswag: Can a machine really finish your sentence? In *Proceedings of the 57th Annual Meeting of the Association for Computational Linguistics*. Association for Computational Linguistics, 2019.

Magauiya Zhussip, Dmitriy Shopkhoev, Ammar Ali, and Stamatis Lefkimiatis. Share your attention: Transformer weight sharing via matrix-based dictionary learning. *arXiv preprint arXiv:2508.04581*, 2025.

A Appendix

A.1 Derivation of the optimal pair of basis and coefficient matrices

Let us consider the weight matrix \mathbf{W} as a collection of d_1 -dimensional vectors $\mathbf{W} = [\mathbf{w}_1, \dots, \mathbf{w}_{d_2}]$, where $\mathbf{w}_j \in \mathbb{R}^{d_1}$, with $j = 1, \dots, d_2$. We seek to approximate each vector \mathbf{w}_j as a linear combination of basis vectors spanning a lower-dimensional subspace of \mathbb{R}^{d_1} . The optimal basis and coefficients can be found by minimizing the total approximation error:

$$\mathcal{J} = \sum_{j=1}^{d_2} \left\| \mathbf{w}_j - \sum_{i=1}^r c_{i,j} \mathbf{b}_i \right\|_2^2 \equiv \|\mathbf{W} - \mathbf{BC}\|_F^2, \quad (15)$$

subject to the orthogonality constraint $\mathbf{B}^\top \mathbf{B} = \mathbf{I}$, where $\mathbf{B} = [\mathbf{b}_1, \dots, \mathbf{b}_r] \in \mathbb{R}^{d_1 \times r}$ is the basis matrix, $\mathbf{C} \in \mathbb{R}^{r \times d_2}$ is the coefficient matrix with entries $c_{i,j}$, and $\mathbf{I} \in \mathbb{R}^{r \times r}$ is the identity matrix.

To solve this problem, we first reformulate the objective \mathcal{J} into an equivalent form:

$$\mathcal{J} = \text{tr}(\mathbf{W}^\top \mathbf{W}) - 2 \text{tr}(\mathbf{W}^\top \mathbf{B} \mathbf{C}) + \text{tr}(\mathbf{C}^\top \mathbf{B}^\top \mathbf{B} \mathbf{C}). \quad (16)$$

Next, we consider the basis matrix \mathbf{B} as fixed and compute the gradient of the objective w.r.t the matrix coefficient \mathbf{C} as

$$\nabla_{\mathbf{C}} \mathcal{J} = 2\mathbf{B}^\top \mathbf{B} \mathbf{C} - 2\mathbf{B}^\top \mathbf{W}. \quad (17)$$

Setting the gradient to zero and taking into account the constraint $\mathbf{B}^\top \mathbf{B} = \mathbf{I}$, we can recover the optimum matrix coefficient as: $\mathbf{C} = \mathbf{B}^\top \mathbf{W}$. Now, putting back \mathbf{C} in Eq. (16) we get:

$$\begin{aligned} \mathcal{J} &= \text{tr}(\mathbf{W}^\top \mathbf{W}) - 2 \text{tr}(\mathbf{W}^\top \mathbf{B} \mathbf{B}^\top \mathbf{W}) + \text{tr}(\mathbf{W}^\top \mathbf{B} \mathbf{B}^\top \mathbf{B} \mathbf{B}^\top \mathbf{W}) \\ &= \text{tr}(\mathbf{W}^\top \mathbf{W}) - \text{tr}(\mathbf{W}^\top \mathbf{B} \mathbf{B}^\top \mathbf{W}) \quad (\text{from the constraint } \mathbf{B}^\top \mathbf{B} = \mathbf{I}) \\ &= \text{tr}(\mathbf{W}^\top \mathbf{W}) - \text{tr}(\mathbf{B}^\top \mathbf{W} \mathbf{W}^\top \mathbf{B}). \end{aligned} \quad (18)$$

Based on this we can recover the optimum basis matrix \mathbf{B} as the maximizer of the constrained problem:

$$\mathbf{B}^* = \arg \max_{\mathbf{B}} \text{tr}(\mathbf{B}^\top \mathbf{W} \mathbf{W}^\top \mathbf{B}) \text{ s.t. } \mathbf{B}^\top \mathbf{B} = \mathbf{I}. \quad (19)$$

The above maximization problem enjoys a closed-form solution Fan (1949), which is fully defined by the eigenvalues of the matrix $\mathbf{P} = \mathbf{W} \mathbf{W}^\top$. Specifically, the matrix $\mathbf{P} \in \mathbb{R}^{d_1 \times d_1}$, which is symmetric and positive semi-definite, admits the eigenvalue decomposition $\mathbf{P} = \mathbf{U} \mathbf{\Lambda} \mathbf{U}^\top$, with $\mathbf{U} \in \mathbb{R}^{d_1 \times d_1}$ holding the eigenvectors of \mathbf{P} in its columns. Then, the maximizer of Eq. (19) is recovered as $\mathbf{B}^* = \mathbf{U}_r$ where $\mathbf{U}_r \in \mathbb{R}^{d_1 \times r}$ is a reduced version of \mathbf{U} formed with the r eigenvectors corresponding to the largest eigenvalues of \mathbf{P} . A useful observation is that the eigenvectors of \mathbf{P} exactly match the left-singular vectors of $\mathbf{W} \in \mathbb{R}^{d_1 \times d_2}$. Indeed, if \mathbf{W} admits the singular value decomposition $\mathbf{W} = \mathbf{U} \mathbf{\Sigma} \mathbf{V}^\top$, then we have that: $\mathbf{P} = \mathbf{W} \mathbf{W}^\top = \mathbf{U} \mathbf{\Sigma}^2 \mathbf{U}^\top \equiv \mathbf{U} \mathbf{\Lambda} \mathbf{U}^\top$, with $\mathbf{\Lambda} = \mathbf{\Sigma}^2$. Therefore, instead of performing the eigenvalue decomposition on \mathbf{P} we can recover \mathbf{U} and consequently \mathbf{U}_r by computing the SVD of \mathbf{W} .

Finally, we can compute the optimum coefficient matrix as:

$$\begin{aligned} \mathbf{C}^* &= (\mathbf{B}^*)^\top \mathbf{W} = \mathbf{U}_r^\top \mathbf{W} \\ &= \mathbf{U}_r^\top \underbrace{[\mathbf{U}_r \quad \mathbf{U}_{d-r}]}_{\mathbf{U}} \underbrace{[\mathbf{\Sigma}_r \quad \mathbf{O}_{r \times (d-r)}]}_{\mathbf{\Sigma}} \underbrace{[\mathbf{V}_r^\top \quad \mathbf{V}_{d-r}^\top]}_{\mathbf{V}^\top} \\ &= [\mathbf{I}_{r \times r} \quad \mathbf{O}_{r \times (d-r)}] \begin{bmatrix} \mathbf{\Sigma}_r \mathbf{V}_r^\top \\ \mathbf{\Sigma}_{d-r} \mathbf{V}_{d-r}^\top \end{bmatrix} \\ &= \mathbf{\Sigma}_r \mathbf{V}_r^\top, \end{aligned} \quad (20)$$

where $\mathbf{V}_r \in \mathbb{R}^{d_2 \times r}$ is a reduced version of \mathbf{V} formed with the r right singular vectors of \mathbf{W} that correspond to its top- r singular values, which are kept in the diagonal matrix $\mathbf{\Sigma}_r \in \mathbb{R}^{r \times r}$.

A.2 Data-Aware Low-Rank Weight Approximation

While the low-rank approximation of the weights \mathbf{W} has been extensively used for compression tasks, in practice is not well suited to LLMs and it can lead to a severe drop of their performance. Several recent works have suggested that instead of approximating the weights \mathbf{W} with a low-rank matrix, a more efficient strategy is to model the weight activations, $\mathbf{Z} = \mathbf{X} \mathbf{W}$, as low-rank. Here, the matrix $\mathbf{X} = [\mathbf{x}_1 \quad \dots \quad \mathbf{x}_N]^\top \in \mathbb{R}^{N \times d}$ holds in its rows the d -dimensional input vectors \mathbf{x}_n with $n = 1, \dots, N$, which play the role of calibration data. Under this modeling framework, we can approximate the matrix weights \mathbf{W} as the minimizer of the following problem:

$$\tilde{\mathbf{W}}^* = \arg \min_{\mathbf{W}} \|\mathbf{X} \mathbf{W} - \mathbf{X} \tilde{\mathbf{W}}\|_F \text{ s.t. } \text{rank}(\mathbf{X} \tilde{\mathbf{W}}) = r. \quad (21)$$

Let us now consider $\mathbf{Y} = \mathbf{XL}^{-1} \in \mathbb{R}^{N \times d_1}$ to be a semi-orthogonal matrix (column-orthogonal matrix), that is $\mathbf{Y}^\top \mathbf{Y} = \mathbf{I}_{d_1}$, which is obtained by linearly transforming the matrix \mathbf{X} using a non-singular matrix $\mathbf{L} \in \mathbb{R}^{d_1 \times d_1}$. Here we assume that $N \geq d$ and the matrix \mathbf{X} is of full rank. We note that there are different ways we can achieve this column-orthogonalization of \mathbf{X} . Among them we can employ the QR/SVD decomposition on \mathbf{X} and the Cholesky/Eigen-value decomposition on $\mathbf{X}^\top \mathbf{X}$ to compute a proper linear transformation \mathbf{L} . By using the representation $\mathbf{X} = \mathbf{YL}$ we can rewrite the problem of Eq. (21) as:

$$\tilde{\mathbf{W}}^* = \arg \min_{\tilde{\mathbf{W}}} \|\mathbf{YLW} - \mathbf{YL}\tilde{\mathbf{W}}\|_F \text{ s.t. rank}(\mathbf{YL}\tilde{\mathbf{W}}) = r. \quad (22)$$

To solve the above minimization problem we first note that due to the orthonormal columns of \mathbf{Y} , it can be expressed in the equivalent form:

$$\tilde{\mathbf{W}}^* = \arg \min_{\tilde{\mathbf{W}}} \|\Delta - \mathbf{L}\tilde{\mathbf{W}}\|_F \text{ s.t. rank}(\mathbf{L}\tilde{\mathbf{W}}) = r, \quad (23)$$

where $\Delta = \mathbf{LW}$. Next, we introduce the auxiliary matrix $\tilde{\Delta} = \mathbf{L}\tilde{\mathbf{W}}$ and the problem in Eq. (23) becomes:

$$\tilde{\Delta}^* = \arg \min_{\tilde{\Delta}} \|\Delta - \tilde{\Delta}\|_F \text{ s.t. rank}(\tilde{\Delta}) = r, \quad (24)$$

which is the orthogonal projection of Δ to the space of r -rank matrices. Given that $\tilde{\Delta}^* = \mathbf{L}\tilde{\mathbf{W}}^*$ and \mathbf{L} is invertible, we can now recover $\tilde{\mathbf{W}}^* = \mathbf{L}^{-1}\tilde{\Delta}^*$.

To conclude, if Δ admits the singular value decomposition $\Delta = \mathbf{U}\Sigma\mathbf{V}^\top$, then the optimal r -rank approximation of \mathbf{W} that minimizes the loss in Eq. (21) can be written in the form:

$$\tilde{\mathbf{W}} = \mathbf{BC} = \underbrace{\mathbf{L}^{-1}\mathbf{U}_r}_{\mathbf{B}} \underbrace{\Sigma_r \mathbf{V}_r^\top}_{\mathbf{C}}. \quad (25)$$

We note that in this case, unlike the direct weight low-rank approximation, the matrix $\mathbf{B} = \mathbf{L}^{-1}\mathbf{U}_r$ does not correspond to a basis of a subspace of \mathbb{R}^{d_1} , since its columns are no longer orthonormal, that is $\mathbf{B}^\top \mathbf{B} = \mathbf{U}_r^\top (\mathbf{L}\mathbf{L}^\top)^{-1} \mathbf{U}_r \neq \mathbf{I}$.

A.3 Pseudo Algorithm of the Proposed Method

Goal. Given a weight matrix $\mathbf{W} \in \mathbb{R}^{d_1 \times d_2}$ and a small calibration set $\mathbf{X} \in \mathbb{R}^{N \times d_1}$, compute an activation-aware sparsedictionary factorization $\mathbf{W} \approx \widehat{\mathbf{W}} = \mathbf{DS}$ under a target compression ratio. The procedure consists of whitening the activation objective, alternating sparse coding and dictionary updates on the whitened weights, and a final de-whitening step.

(1) Calibration and whitening. Compute an invertible transform $\mathbf{L} \in \mathbb{R}^{d_1 \times d_1}$ (e.g., via QR/SVD of \mathbf{X} or Cholesky of $\mathbf{X}^\top \mathbf{X}$) such that $\mathbf{Y} = \mathbf{XL}^{-1}$ has orthonormal columns ($\mathbf{Y}^\top \mathbf{Y} = \mathbf{I}$). Left-multiply \mathbf{W} to obtain the whitened weights $\mathbf{W}_L = \mathbf{LW}$. Whitening converts the data-aware loss $\|\mathbf{XW} - \mathbf{X}\widehat{\mathbf{W}}\|_F^2$ into a standard Frobenius objective $\|\mathbf{W}_L - \mathbf{DL}\mathbf{S}\|_F^2$ that is amenable to dictionary learning.

(2) Initialization. Initialize the whitened dictionary $\mathbf{D}_L^{(0)} \in \mathbb{R}^{d_1 \times k}$ (e.g., random permutation of columns of \mathbf{W}) and set $\mathbf{S}^{(0)} = 0$. The pair (k, s) is set from the target compression ratio via Eq. 13 optionally using the fixed ratio $\rho = k/s$.

(3) Alternating minimization. Repeat for $t = 1, \dots, T$: *(a) Sparse coding.* For each column j , solve

$$\mathbf{s}_j^{(t)} \in \arg \min_{\|\mathbf{s}\|_0 \leq s} \|(\mathbf{W}_L)_{:,j} - \mathbf{D}_L^{(t-1)}\mathbf{s}\|_2^2,$$

using OMP (greedy selection with orthogonal residual updates) to enforce exactly s nonzeros per column. *(b) Dictionary update.* For each atom i , collect its support $\Omega_i = \{j : s_{i,j}^{(t)} \neq 0\}$ and form the residual on

those columns:

$$\mathbf{R}_i = \mathbf{W}_L[:, \Omega_i] - \sum_{\ell \neq i} \mathbf{D}_{\mathbf{L}, \ell}^{(t-1)} \mathbf{s}_{\ell, \Omega_i}^{(t)}.$$

Update $(\mathbf{D}_{\mathbf{L}, i}^{(t)}, \mathbf{s}_{i, \Omega_i}^{(t)})$ by the best rank-1 approximation $\mathbf{R}_i \approx \mathbf{u} \sigma \mathbf{v}^\top$ (set $/m D_{L, i}^{(t)} \leftarrow \mathbf{u}$, $\mathbf{s}_{i, \Omega_i}^{(t)} \leftarrow \sigma \mathbf{v}^\top$). This preserves the current sparsity pattern while reducing the residual. Iterate atoms sequentially. Stop when the maximum iteration T is reached or when the relative improvement falls below a tolerance.

(4) De-whitening and packing. Map the dictionary back to activation space via $\mathbf{D}_a = \mathbf{L}^{-1} \mathbf{D}_{\mathbf{L}}^{(T)}$ and set $\widetilde{\mathbf{W}} = \mathbf{D}_a \mathbf{S}^{(T)}$. For storage, keep \mathbf{D}_a and the sd_2 nonzero entries of \mathbf{S} in **bf16** along with a packed binary mask $\mathbf{M} \in \{0, 1\}^{k \times d_2}$ for locations (one bit per entry; $\frac{kd_2}{16}$ words). This yields the compression ratio in Appendix A.4 and Eq. 12.

(5) Inference. At runtime, apply $\widetilde{\mathbf{W}}$ as $\text{matmul}(\mathbf{x}, \mathbf{D}_a \mathbf{S})$ with sparsedense kernels. Reuse inner products $\langle \mathbf{x}, \mathbf{D}_{a, :, i} \rangle$ across columns to achieve the complexity in Appendix A.5; the number of active atoms controls the practical speedup.

(6) Cross-layer variant. For a group of layers \mathbf{G} , concatenate weights horizontally $\mathbf{W}_G = [\mathbf{W}_{\ell_1} \cdots \mathbf{W}_{\ell_L}]$ and stack calibration batches vertically to form \mathbf{X}_G . Compute \mathbf{L} from \mathbf{X}_G , run the same alternating procedure on $\mathbf{W}_{L, G} = \mathbf{L} \mathbf{W}_G$ to obtain a single shared \mathbf{D}_a , and slice the corresponding blocks of \mathbf{S}_G back to per-layer coefficients.

A.4 Derivation of the CoSpaDi Compression Ratio

We derive the expression for the compression ratio γ^{SD} of our sparsedictionary (SD) parameterization. Let $\mathbf{W} \in \mathbb{R}^{d_1 \times d_2}$ be factorized as

$$\mathbf{W} \approx \mathbf{D} \mathbf{S}, \quad \mathbf{D} \in \mathbb{R}^{d_1 \times k}, \quad \mathbf{S} \in \mathbb{R}^{k \times d_2},$$

where each column of \mathbf{S} has exactly s nonzeros (*column- s -sparse*). Throughout, we store real values in **bf16** (16 bits) as is common in modern LLMs.

Dense baseline. A dense \mathbf{W} requires $d_1 d_2$ **bf16** values.

Dictionary term. The dictionary \mathbf{D} stores $d_1 k$ **bf16** values.

Sparse codes. Naively, \mathbf{S} would need kd_2 values. Since \mathbf{S} is column- s -sparse, only sd_2 values are stored. For locations, one option is COO: per nonzero we keep a row index and (redundantly) the column index. Because sparsity is fixed per column, column indices can be omitted; keeping only row indices yields sd_2 indices. With 16-bit indices, the total becomes sd_2 values + sd_2 indices = $2sd_2$ 16-bit words. For typical $\rho := k/s = 2$, this equals kd_2 words offering no savings over dense \mathbf{S} storage.

Instead, we use a *bit mask* $\mathbf{M} \in \{0, 1\}^{k \times d_2}$ to mark nonzero positions. This requires kd_2 bits, i.e., $\frac{kd_2}{16}$ 16-bit words after packing. We then store sd_2 **bf16** values for the nonzeros and the packed mask for their positions.

Total and ratio. The SD parameterization thus stores

$$\underbrace{d_1 k}_{\text{dictionary}} + \underbrace{sd_2}_{\text{values}} + \underbrace{\frac{kd_2}{16}}_{\text{mask}}$$

16-bit words. Relative to the dense baseline $d_1 d_2$, the resulting compression ratio is

$$\gamma^{\text{SD}} := 1 - \frac{\underbrace{d_1 k}_{\text{dict. (bf16)}} + \underbrace{sd_2}_{\text{codes (bf16)}} + \underbrace{(kd_2)/16}_{\text{mask (1 bit/entry)}}}{d_1 d_2}.$$

This matches the expression used in the main text and makes explicit the dependence on the two design knobs (k, s) .

Algorithm 1: Pseudo algorithm of the proposed CoSpaDi which consists of two steps: (a) sparse coding to compute the coefficients and (b) sequential dictionary update step.

Input : $\mathbf{W} \in \mathbb{R}^{d_1 \times d_2}$: weight matrix to compress

$\mathbf{X} \in \mathbb{R}^{N \times d_1}$: calibration input data (N samples)

k : dictionary size (number of atoms, $k \geq s$)

s : sparsity level (max nonzeros per column in \mathbf{S})

T : number of K-SVD iterations

Output: $\mathbf{D}_a \in \mathbb{R}^{d_1 \times k}$: activation-aware dictionary

$\mathbf{S} \in \mathbb{R}^{k \times d_2}$: sparse coefficient matrix

$\tilde{\mathbf{W}} = \mathbf{D}_a \mathbf{S}$: compressed weight matrix

Compute $\mathbf{L} \in \mathbb{R}^{d_1 \times d_1}$ such that $\mathbf{Y} = \mathbf{XL}^{-1}$ satisfies $\mathbf{Y}^\top \mathbf{Y} = \mathbf{I}_{d_1}$;

% e.g., via QR: $\mathbf{X} = \mathbf{QR} \Rightarrow \mathbf{L} = \mathbf{R}$

% e.g., via Cholesky: $\mathbf{X}^\top \mathbf{X} = \mathbf{C}^\top \mathbf{C} \Rightarrow \mathbf{L} = \mathbf{C}$

$\mathbf{W}_L \leftarrow \mathbf{LW}$;

Initialize $\mathbf{D}_L^{(0)} \in \mathbb{R}^{d_1 \times k}$ with random Gaussian or SVD-based atoms;

Initialize $\mathbf{S}^{(0)} \in \mathbb{R}^{k \times d_2}$ as zero matrix;

for $t = 1$ **to** T **do**

for $j = 1$ **to** d_2 **do**

$\mathbf{s}_j^{(t)} \leftarrow \arg \min_{\|\mathbf{s}\|_0 \leq s} \left\| \mathbf{W}_{L,j} - \mathbf{D}_L^{(t-1)} \mathbf{s} \right\|_2^2$;

 % Solve via OMP, LASSO, or thresholding

end

for $i = 1$ **to** k **do**

$\Omega_i \leftarrow \{j \mid s_{i,j}^{(t)} \neq 0\}$;

if $\Omega_i \neq \emptyset$ **then**

$\mathbf{R}_i \leftarrow \mathbf{W}_L[:, \Omega_i] - \sum_{l \neq i} \mathbf{d}_{L,l}^{(t-1)} \mathbf{s}_{l,\Omega_i}^{(t)}$;

$[\mathbf{u}, \sigma, \mathbf{v}] \leftarrow$ rank-1 SVD of \mathbf{R}_i ;

$\mathbf{d}_{L,i}^{(t)} \leftarrow \mathbf{u}$;

$\mathbf{s}_{i,\Omega_i}^{(t)} \leftarrow \sigma \cdot \mathbf{v}^\top$;

end

end

end

$\mathbf{D}_a \leftarrow \mathbf{L}^{-1} \mathbf{D}_L^{(T)}$;

$\tilde{\mathbf{W}} \leftarrow \mathbf{D}_a \mathbf{S}^{(T)}$;

return $\mathbf{D}_a, \mathbf{S}^{(T)}, \tilde{\mathbf{W}}$;

A.5 Low-rank and CoSpaDi Inference Complexity

Here we derive the multiplication complexity for the original weight, SVD-compressed weight, and dictionary-learning (k-SVD) compression. We count multiplications only (additions are of the same order). Let $\mathbf{W} \in \mathbb{R}^{d_1 \times d_2}$ be a projection matrix in some layer and $\mathbf{X} \in \mathbb{R}^{N \times d_1}$ be an input feature map; then a dense product $\mathbf{Y} = \mathbf{XW}$ costs

$$O_{\text{baseline}} = Nd_1d_2. \quad (26)$$

For low-rank, in particular, SVD compression with rank r the projection matrix is approximated with two matrices $\mathbf{W} \approx \mathbf{UV}$ with $\mathbf{U} \in \mathbb{R}^{d_1 \times r}$ and $\mathbf{V} \in \mathbb{R}^{r \times d_2}$, resulting in the following complexity:

$$O_{LR} = Nd_1r + Nrd_2 = Nr(d_1 + d_2). \quad (27)$$

Sparse dictionary (SD) learning similarly represents $\mathbf{W} \approx \mathbf{DS}$ with dictionary $\mathbf{D} \in \mathbb{R}^{d_1 \times k}$ of k atoms and sparse coefficient matrix $\mathbf{S} \in \mathbb{R}^{k \times d_2}$. Omitting sparsity of \mathbf{S} will result in:

$$O_{SD,dense} = Nd_1k + Nkd_2 = Nk(d_1 + d_2). \quad (28)$$

Taking into account that each column \mathbf{s}_j of \mathbf{S} is s -sparse, the (i, j) element of $\mathbf{Y} = \mathbf{XDS}$ is

$$y_{i,j} = \sum_{k=1}^K \mathbf{S}_{k,j} \langle \mathbf{X}_{i,:}, \mathbf{D}_{:,k} \rangle = \sum_{k \in \mathbf{S}_j} \mathbf{S}_{k,j} \langle \mathbf{X}_{i,:}, \mathbf{D}_{:,k} \rangle, \quad (29)$$

where $S_j = \text{supp}(s_j)$ and $|\mathbf{S}_j| = s$. The overall sparse complexity depends on whether the inner products $\langle \mathbf{X}_{i,:}, \mathbf{D}_{:,k} \rangle$ are reused across columns. With the most efficient way with reuse letting $\mathbf{U} = \bigcup_{j=1}^{d_2} S_j$ and $K_{active} = |U|$ we have:

$$O_{SD,sparse-reuse} = Nd_1K_{active} + Nsd_2, \quad s \leq K_{active} \leq \min(K, sd_2). \quad (30)$$

With proposed truncation of 2-bits in mantissa we can omit term for storing indices of nonzero elements in \mathbf{S} resulting in corrected compression ratio:

$$\hat{\gamma}^{SD} = 1 - \frac{d_1k + sd_2}{d_1d_2}$$

The rank for the low-rank decomposition could be estimated from the compression ratio with the following equation:

$$r = \frac{(1 - \hat{\gamma}^{LR})d_1d_2}{d_1 + d_2}$$

For sparse dictionary based method we defined $\rho = k/s$ and, thus we can estimate both k and s in the following way:

$$k = \frac{(1 - \hat{\gamma}^{SD})d_1d_2}{d_1 + \frac{d_2}{\rho}}, \quad s = \frac{k}{\rho}.$$

Under the same compression ratio for both SVD and CoSpaDi we obtain exactly the same complexity:

$$\begin{aligned} O_{LR} &= Nr(d_1 + d_2) = N(1 - \hat{\gamma}^{LR})d_1d_2 \\ O_{SD} &= Nd_1k + Nsd_2 = N(d_1k + d_2 \frac{k}{\rho}) = Nk(d_1 + \frac{d_2}{\rho}) = N \frac{(1 - \hat{\gamma}^{SD})d_1d_2}{d_1 + \frac{d_2}{\rho}} (d_1 + \frac{d_2}{\rho}) = N(1 - \hat{\gamma}^{SD})d_1d_2 \\ O_{LR} &= O_{SD} = N(1 - \hat{\gamma}^{SD})d_1d_2. \end{aligned} \quad (31)$$

While, theoretical complexity is the same, in practice inference time depends on the sparsity structure (K_{active}), indexing overhead, and kernel efficiency, as can be observed from Figs. 5, 6 and 7.

A.6 More Benchmarks

We additionally evaluate CoSpaDi and SVD-LLM on the Qwen model family using a set of more recent reasoning-oriented benchmarks. Table 6 reports results for Qwen3-8B and Qwen3-14B across several compression ratios. Overall, CoSpaDi matches or improves upon the SVD-LLM baseline on most benchmarks and settings, indicating that sparse dictionary learning provides a stronger compression-quality trade-off than low-rank factorization beyond the standard evaluation suite.

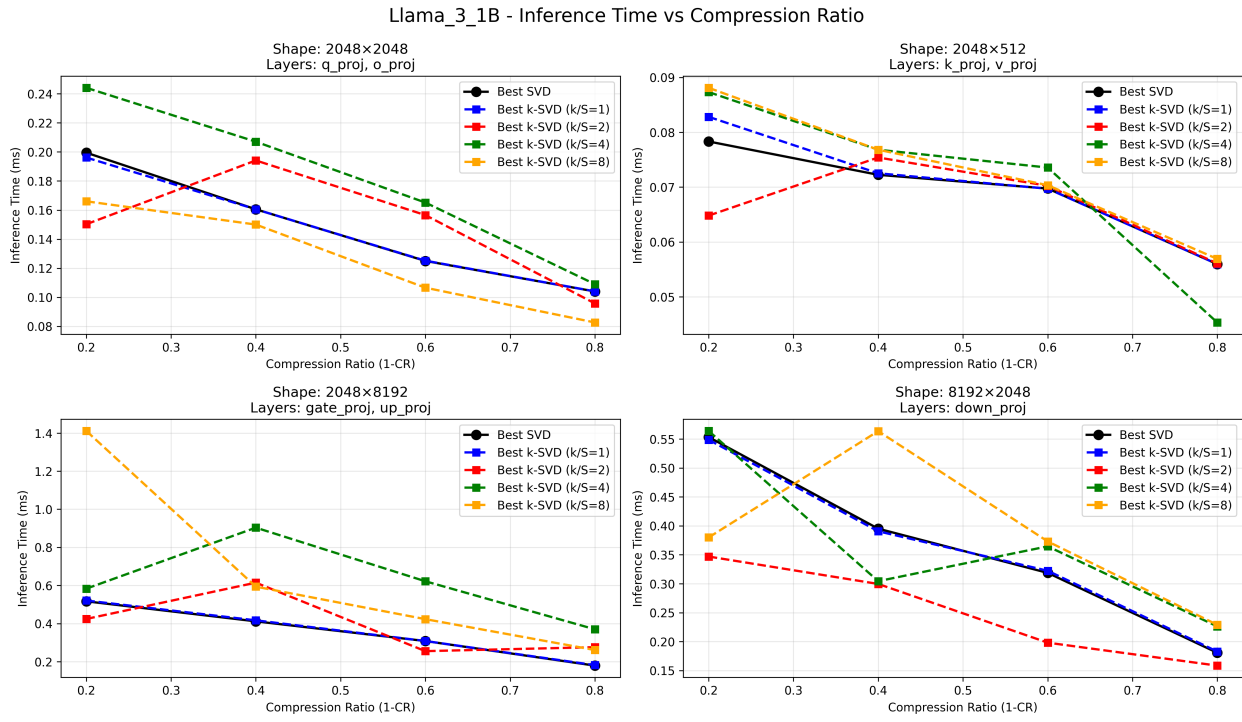


Figure 5: Inference time for different projection layers of Llama3.2 1B for different compression ratios and k/s ratios on A100

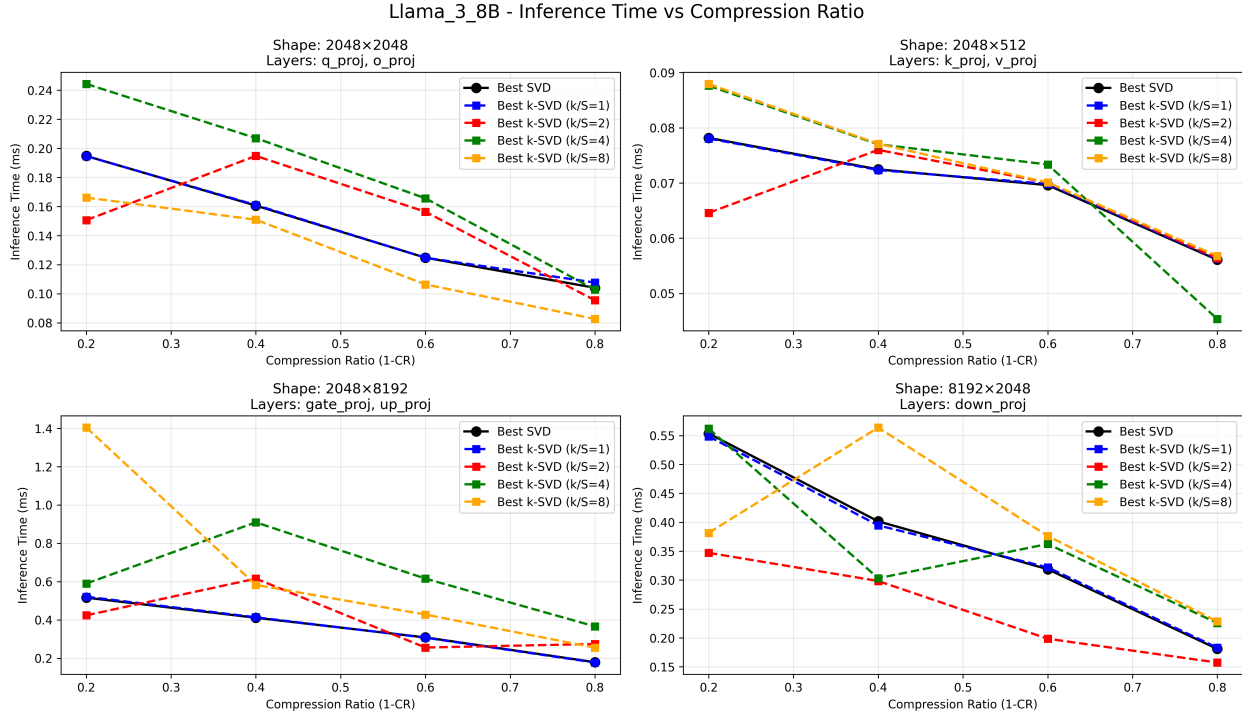


Figure 6: Inference time for different projection layers of Llama3 8B for different compression ratios and k/s ratios on A100

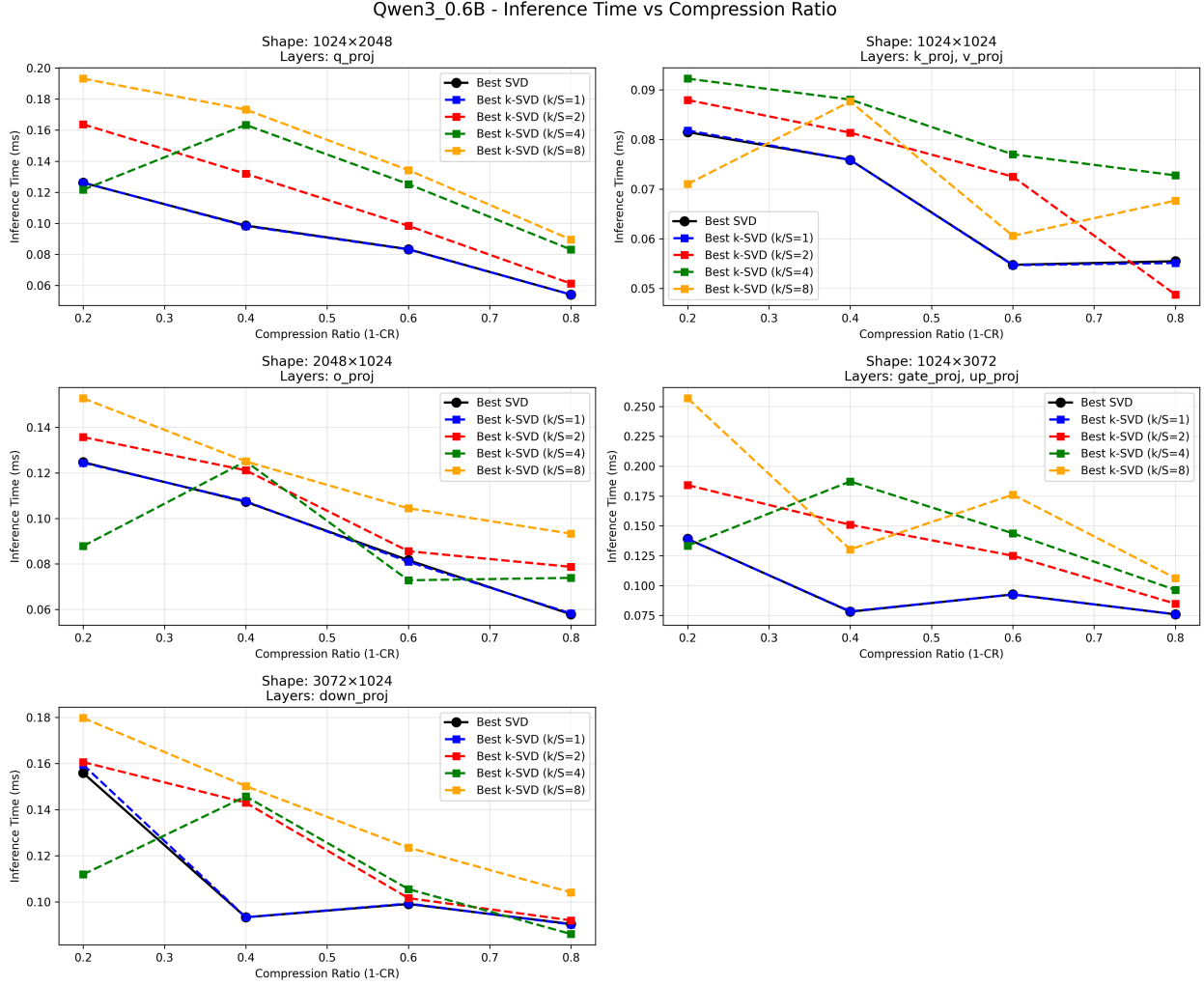


Figure 7: Inference time for different projection layers of Qwen3 0.6B for different compression ratios and k/s ratios on A100

A.7 K-SVD and Power Iteration Analysis

We conducted ablation studies to assess the effect of the number of K-SVD iterations and power iterations on performance using Llama3.2-1B with fixed $\rho = 2$. The left plot in Fig. 8 shows that average accuracy stabilizes after roughly 50 K-SVD iterations, while perplexity continues to decrease slightly before flattening out. The right plot of Fig. 8 indicates that very few power iterations are sufficient for stable convergence: performance improves sharply up to around 5 iterations, after which additional iterations yield minimal benefit. Based on these results, we fixed the number of K-SVD iterations to 60 and power iterations to 8 in our final experiments, which provides a good balance between accuracy, perplexity, and computational efficiency.

Table 6: Performance comparison of CoSpaDi vs sota SVD-LLM on Qwen3-8B and Qwen3-14B at different compression levels on different benchmarks. Best results are highlighted with **bold**.

Model	CR	IFEval (%)	BBH (%)	MATH (%)	GPQA (%)	MUSR (%)	MMLU-Pro (%)
Qwen 3 8B	—	39.2	60.9	52.6	36.2	43.1	47.7
SVDLLM	0.2	25.5	41.0	1.1	28.4	39.8	26.3
CoSpaDi	0.2	28.9	45.3	2.0	28.6	42.1	31.5
SVDLLM	0.3	22.9	34.4	1.0	25.6	41.4	18.8
CoSpaDi	0.3	25.2	38.2	1.0	24.8	38.4	22.8
SVDLLM	0.4	22.7	30.2	0.8	23.1	37.7	11.6
CoSpaDi	0.4	26.1	32.7	0.8	26.0	38.1	16.7
Qwen 3 14B	—	43.3	63.2	53.3	38.6	40.7	53.3
SVDLLM	0.2	25.5	50.1	1.6	29.2	41.5	32.7
CoSpaDi	0.2	29.6	54.2	4.2	30.6	40.7	38.9
SVDLLM	0.4	23.0	34.3	1.1	26.4	39.7	12.8
CoSpaDi	0.4	26.6	38.3	1.2	25.5	38.0	15.7

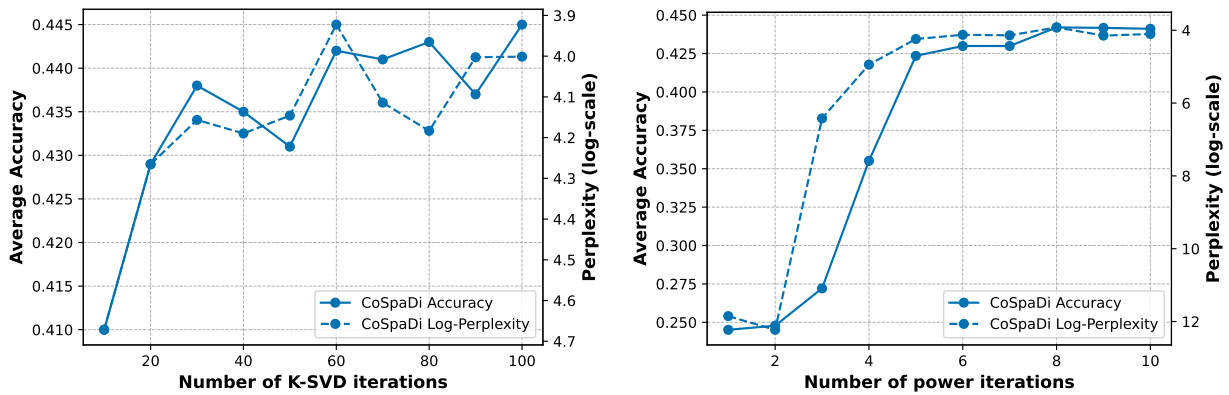


Figure 8: Average benchmark accuracy and WikiText perplexity with respect to the number of K-SVD iterations (left) and the number of power iterations (right) for Llama3.2-1B with $\rho = 2$